TECHNISCHE UNIVERSITÄT BERGAKADEMIE FREIBERG

Die Ressourcenuniversität. Seit 1765.

Mikro- und Meso-Mechanische Simulationen zum Verformungsverhalten von Tongesteinen

Heinz Konietzky
Geotechnical Institute, Chair for Rock Mechanics
TU Bergakademie Freiberg, Germany

Content

1. General comments on micro-mechanical modelling

2. Micro- and meso-mechanical modelling of Opalinus Clay

Method of approach

Macro-mechanical view
(scale: dm, m, km)

„Phenomenological“ concept

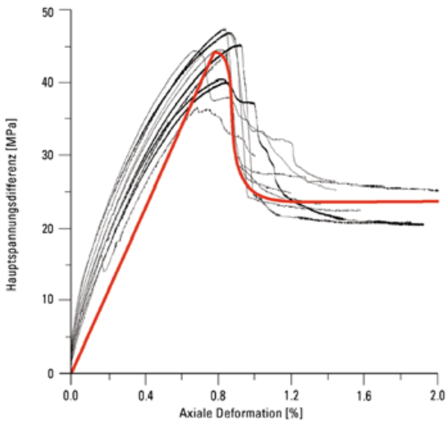

Micro-mechanical view
(scale: nm, µm, mm)

„Physical“ concept

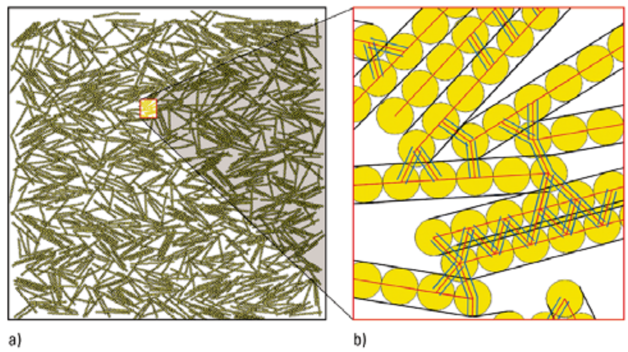

Micromechanical simulation approaches

Choice of simulation approach

deformable polyhedra → Voronoi-bodies

- more physics, more flexible
- computer-intensiv
- potential of numerical instability

stiff spheres → Spheres-Clusters-Clumps

- robust, fast, stable
- physical less flexible

Generation of models

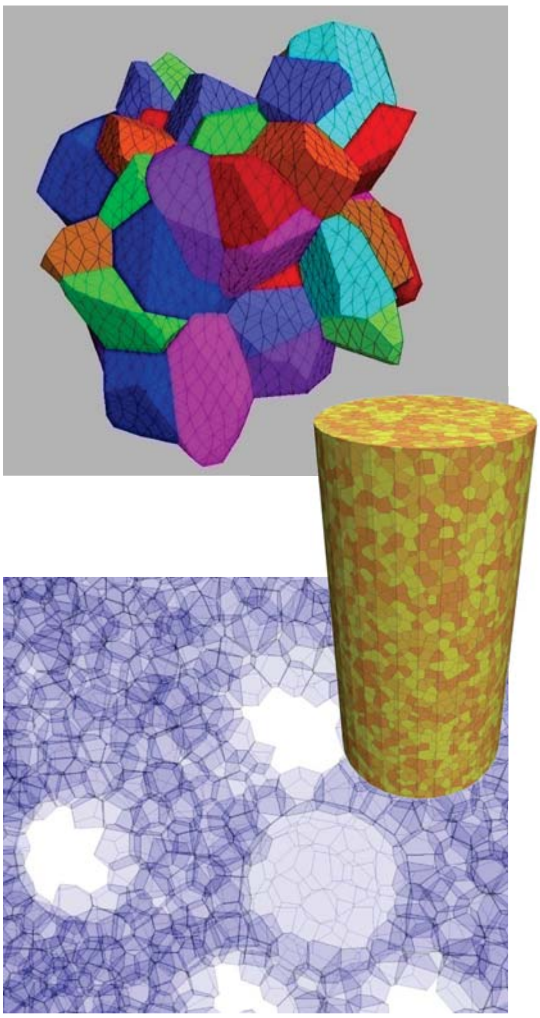

Voronoi Bodies

Spheres – Clumps - Clusters

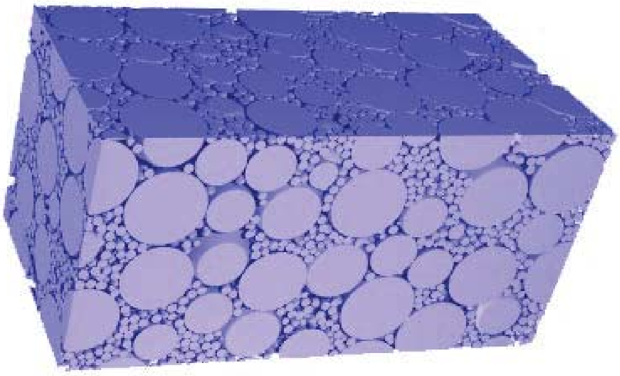

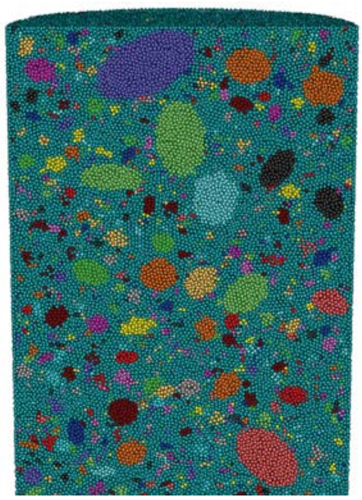

Model set-up based on spheres according to grain size distribution

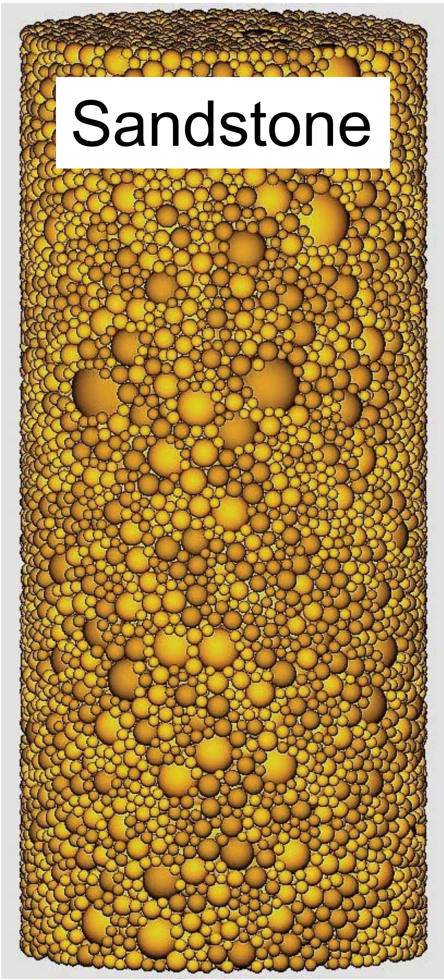

Shear fracture during triaxial testing

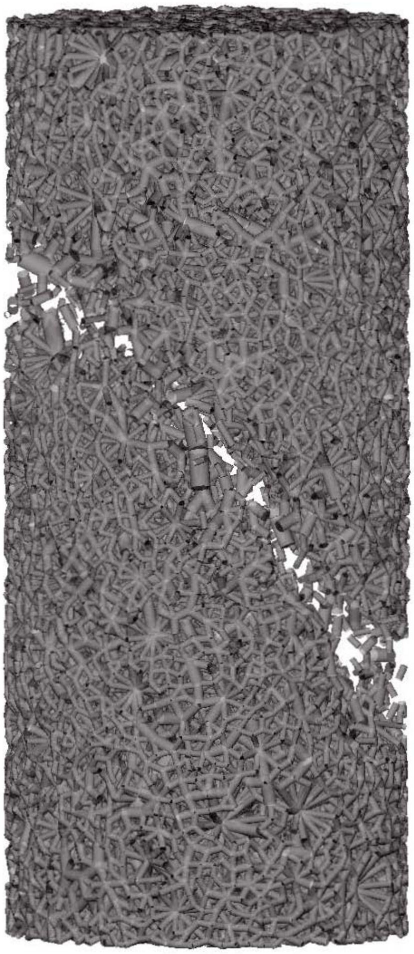

Baumgarten & Konietzky 2013

Sandstone

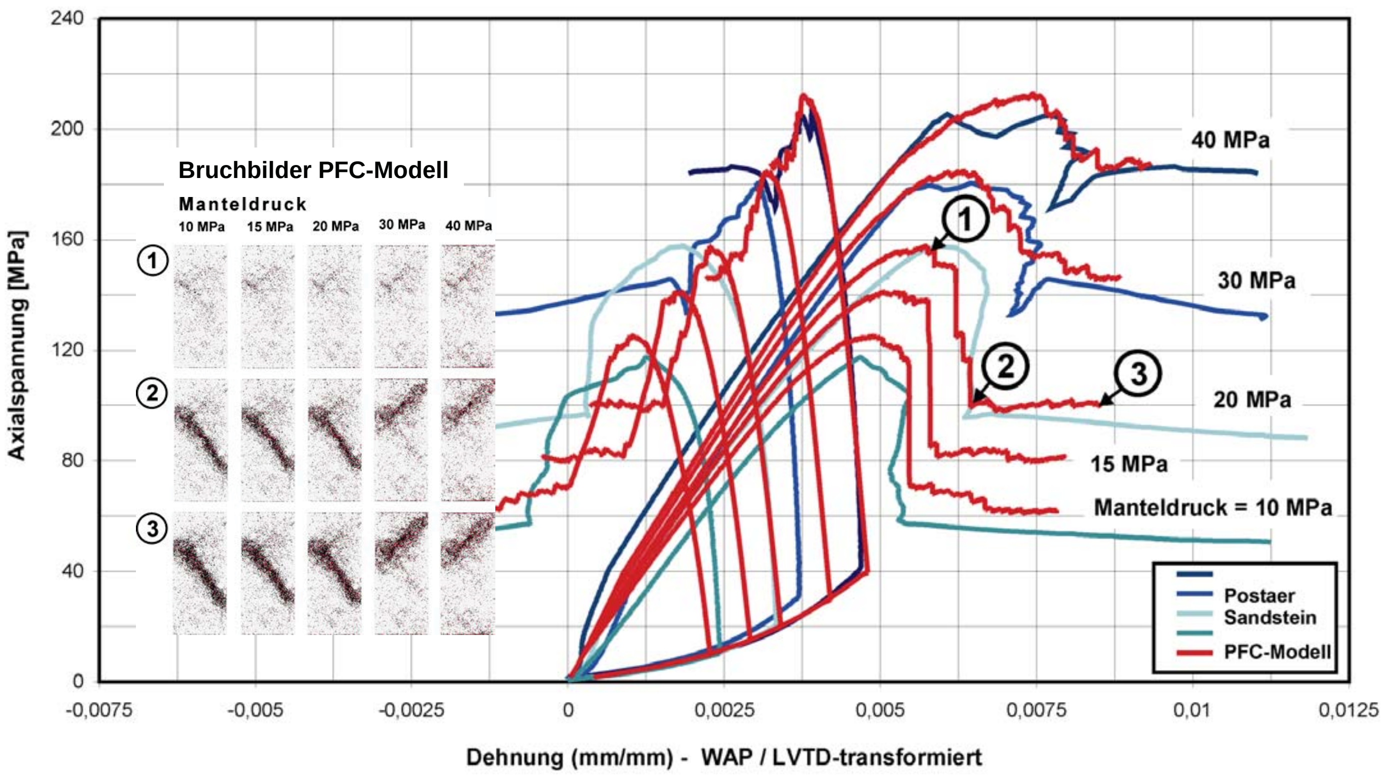

Longitudinal deformation and transverse deformation including hydrostatic pre-loading

Baumgarten & Konietzky 2013

Micromechanical simulation of concrete considering grain size, grain shape + grain and binder properties

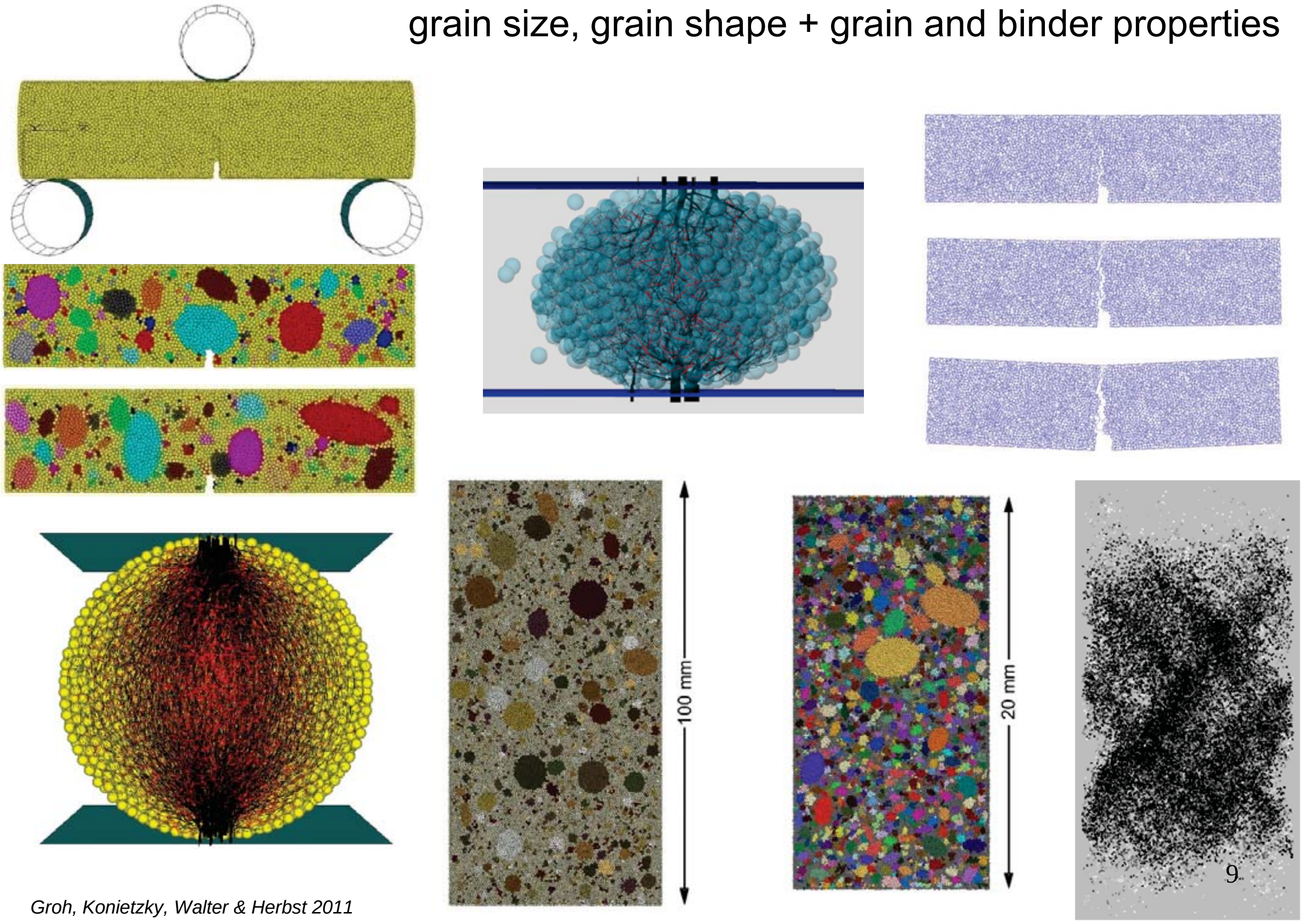

Groh, Konietzky, Walter & Herbst 2011

Fracture toughness test (Mode-I)

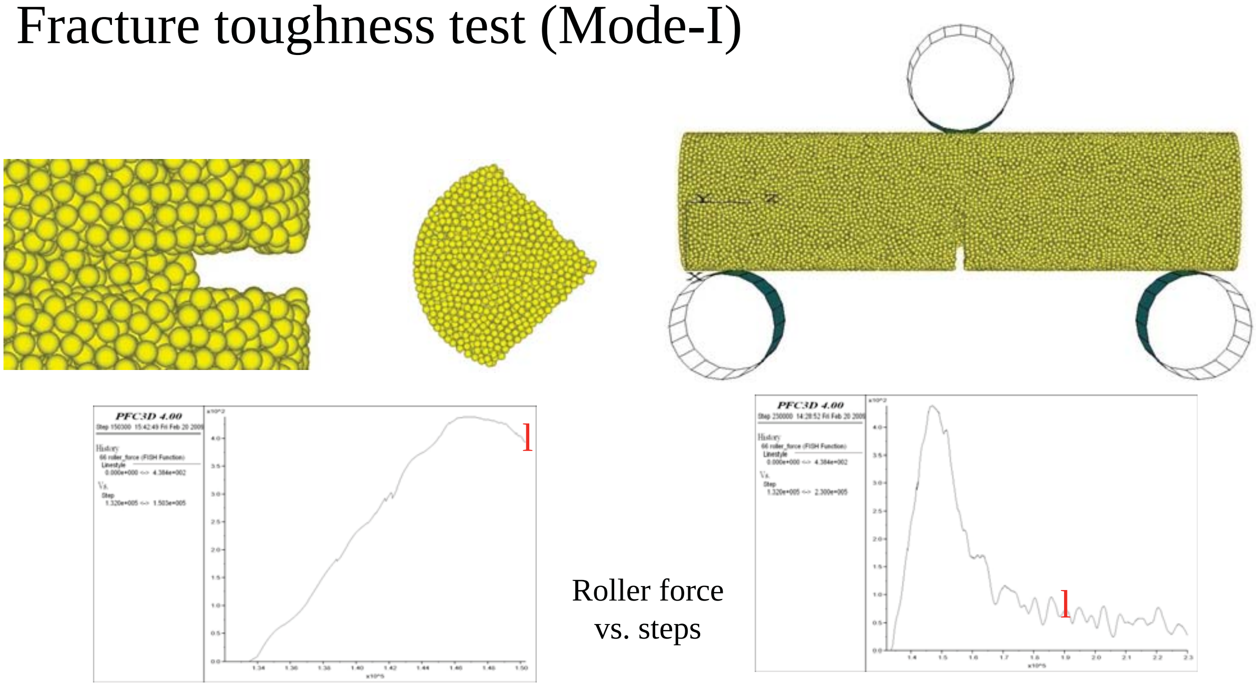

Roller force vs. steps

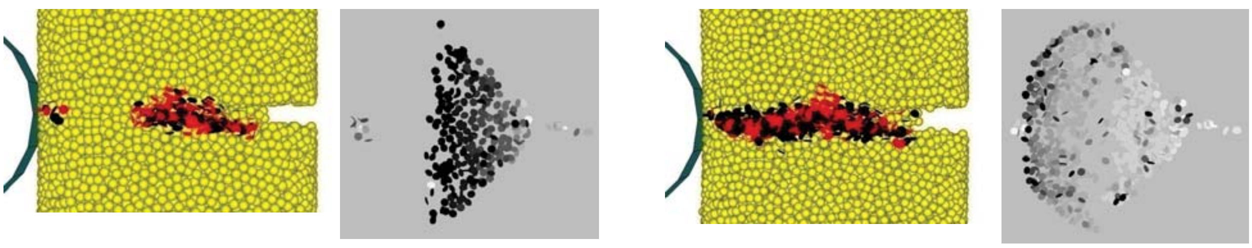

Micro fractures: red/black =t ensile-/shear fracture, dark =l ater

Groh, Konietzky, Walter & Herbst 2011

Micro-mechanical model of single pore of different shape

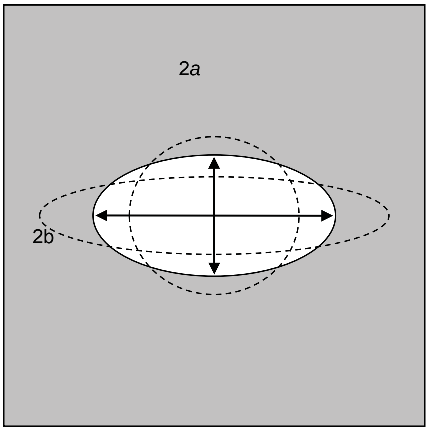

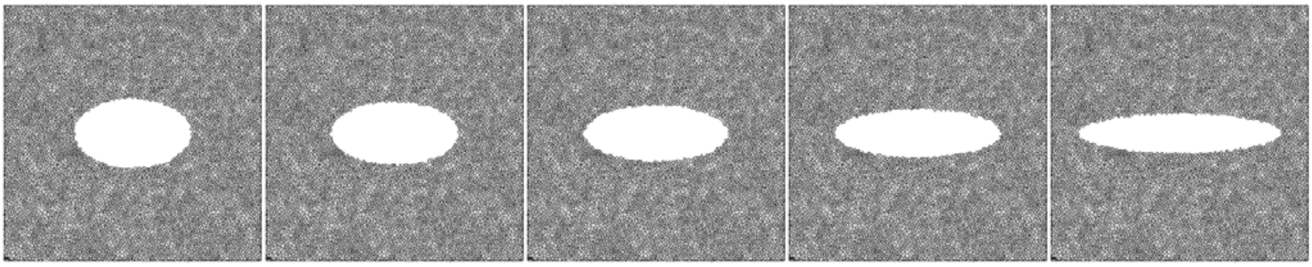

R=0.6 *R*=0.5 *R*=0.4 *R*=0.3 *R*=0.2

Elliptical pores with different aspect ratio

Tan & Konietzky 2013

Random elliptical cracks (S=0.1)

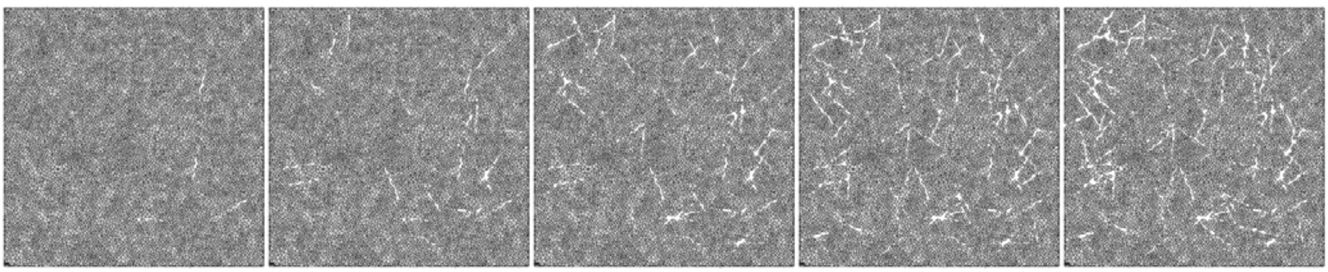

n=0.33% *n*=2.56% *n*=4.54% *n*=6.81% *n*=8.36%

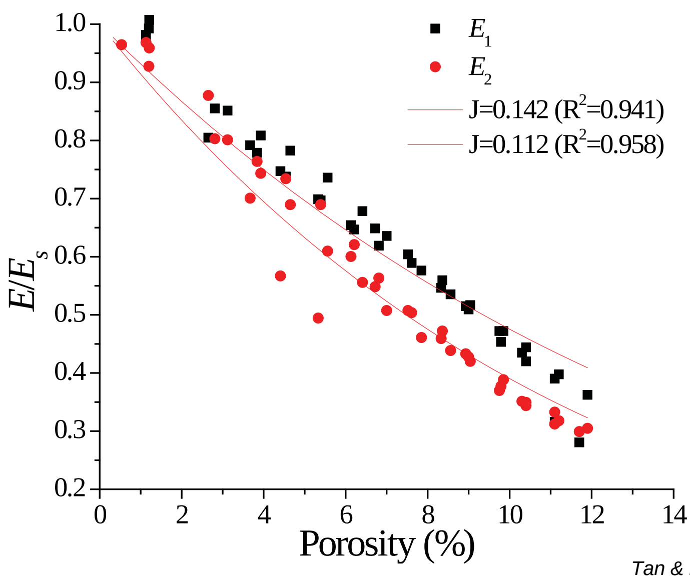

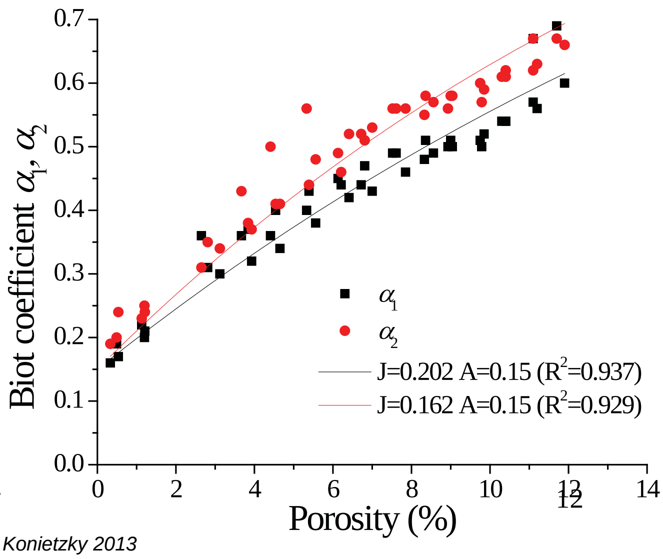

Tan & Konietzky 2013

Tan, Konietzky & Frühwirt 2014

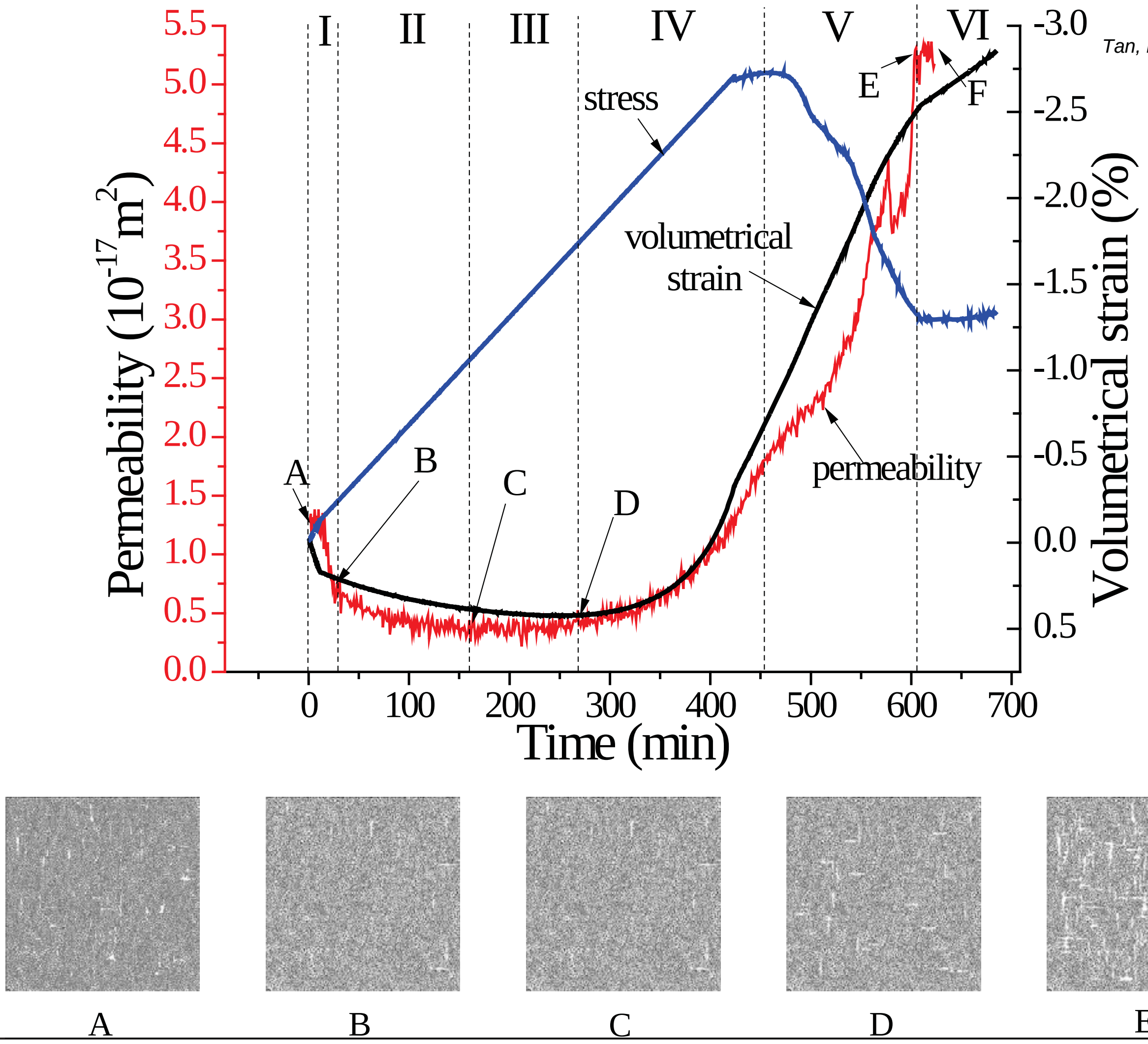

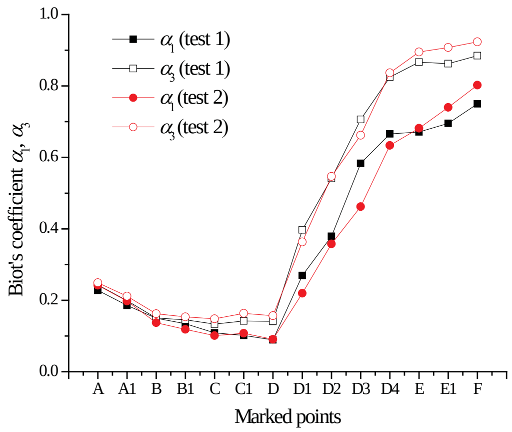

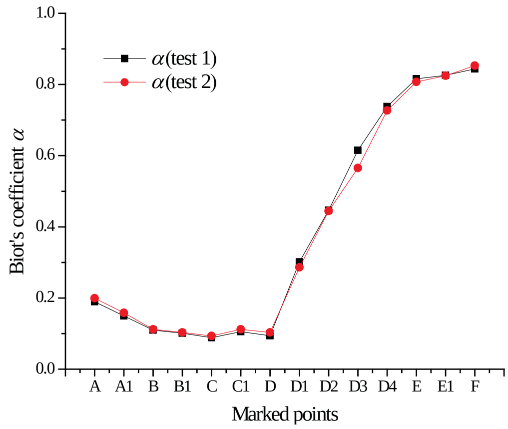

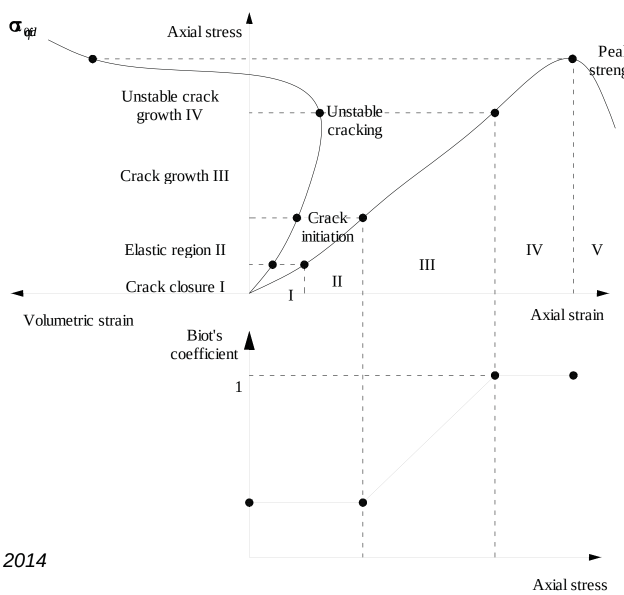

Tan, Konietzky & Frühwirt 2014

Gray level image technique to duplicate microstructure

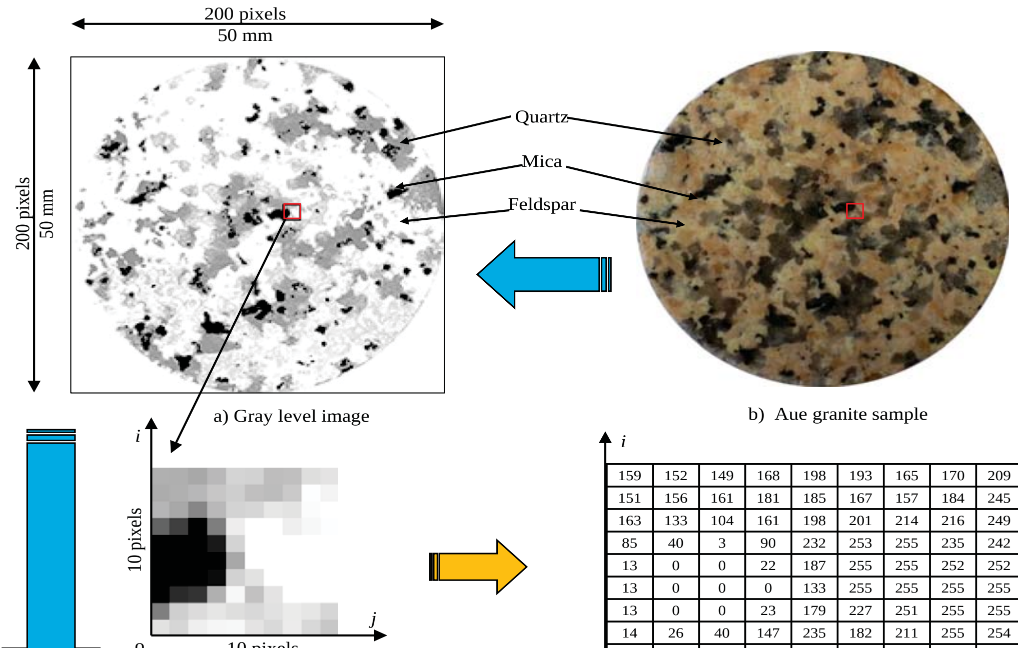

a) Gray level image

b) Aue granite sample

c) Square region

159	152	149	168	198	193	165	170	209	223
151	156	161	181	185	167	157	184	245	244
163	133	104	161	198	201	214	216	249	255
85	40	3	90	232	253	255	235	242	253
13	0	0	22	187	255	255	252	252	255
13	0	0	0	133	255	255	255	255	255
13	0	0	23	179	227	251	255	255	255
14	26	40	147	235	182	211	255	254	253
98	176	205	226	216	195	207	229	220	200
215	213	242	249	239	216	208	225	204	183

d) Matrix of discrete function $f(i, j)$

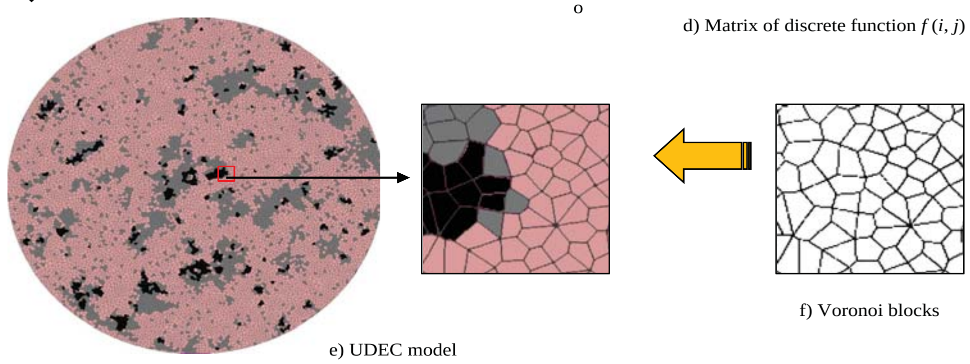

f) Voronoi blocks

e) UDEC model

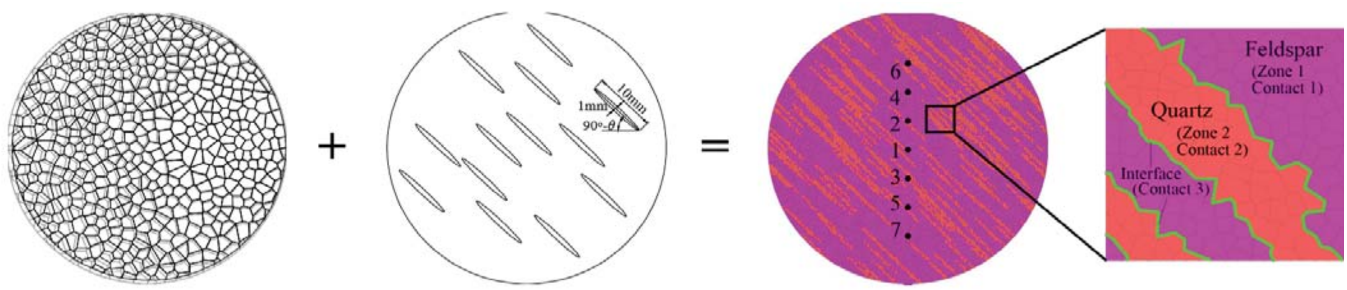

(a) (b) (c)

Micro-structural model of gneiss disc

0° 45° 90°

Schist

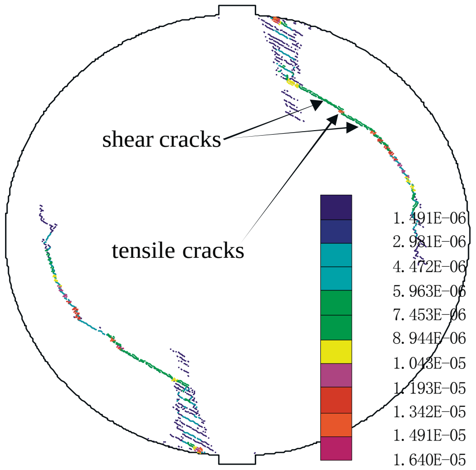

60°

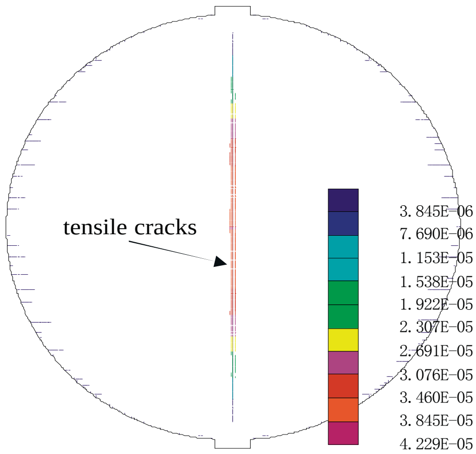

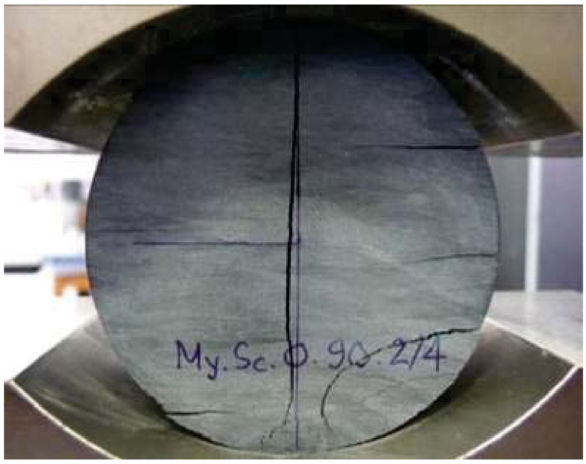

90°

Schist

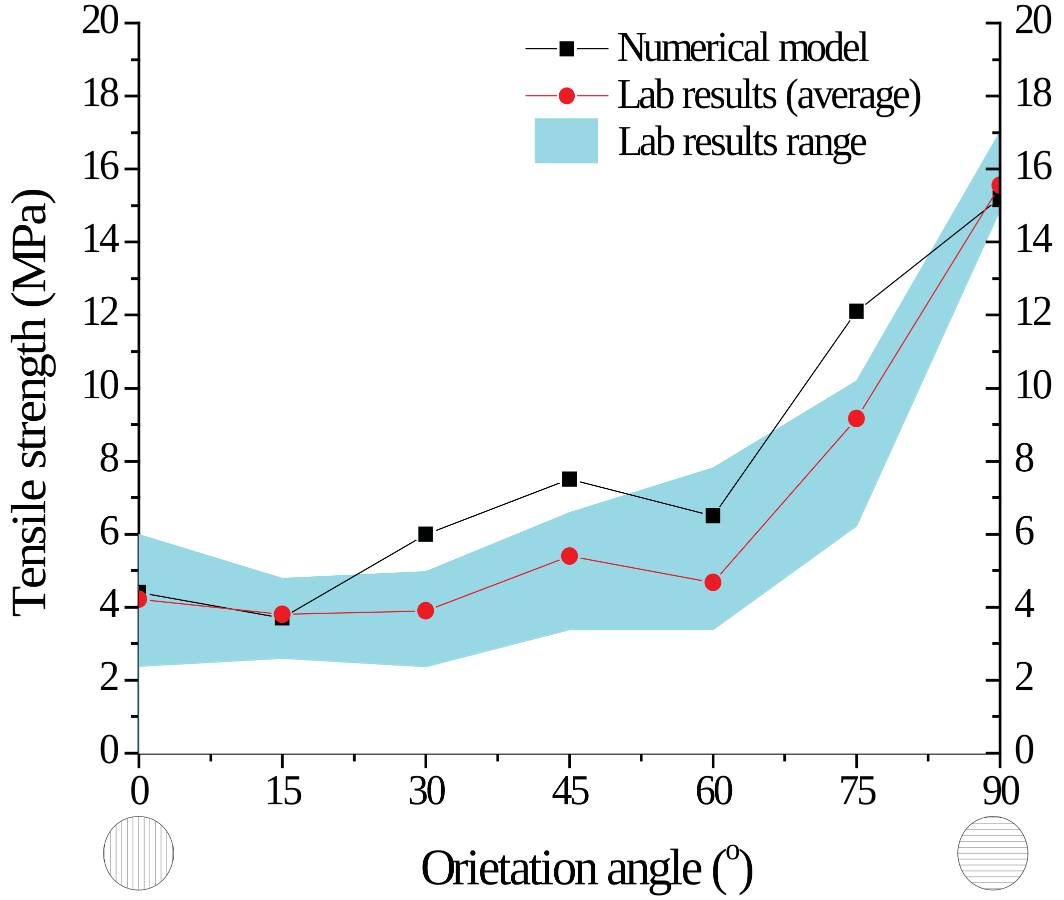

Schist

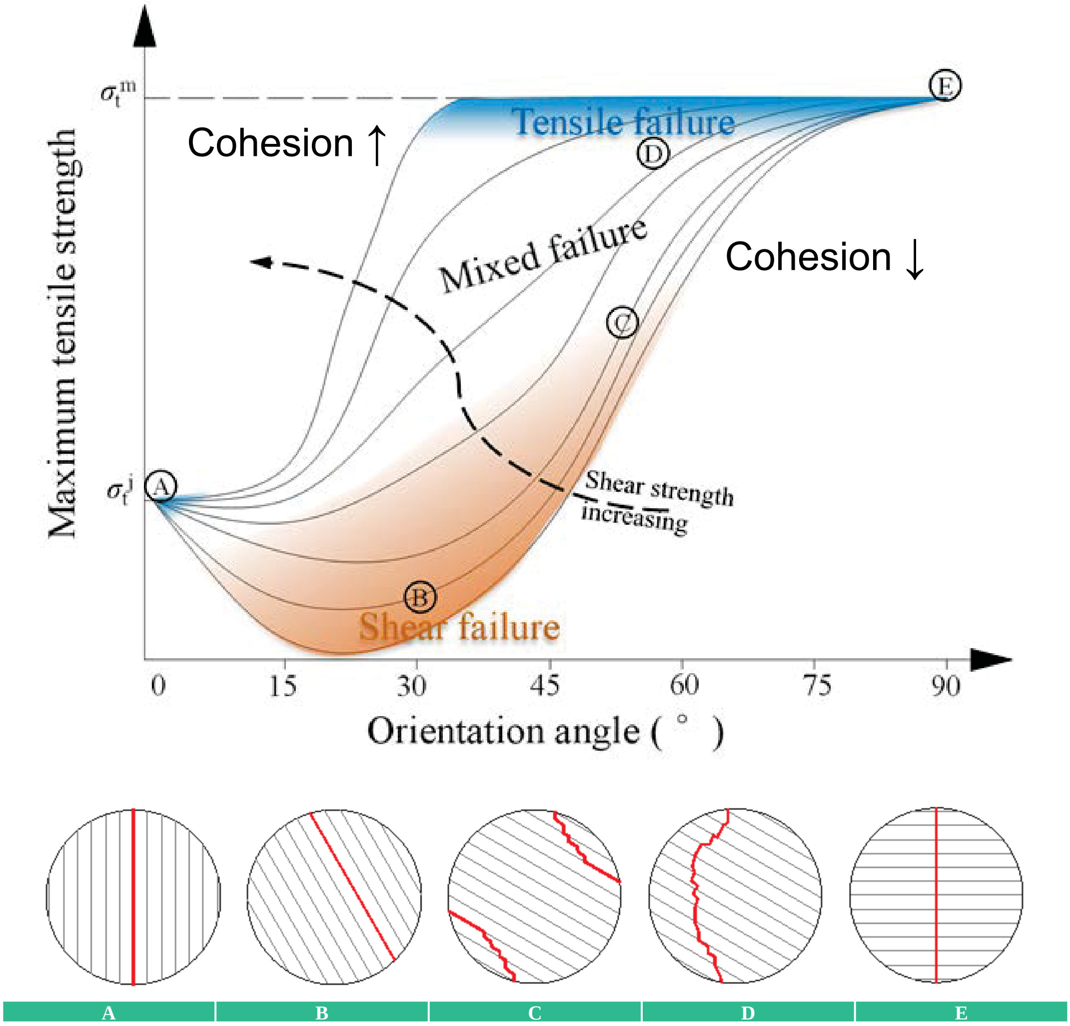

19

Lab test results

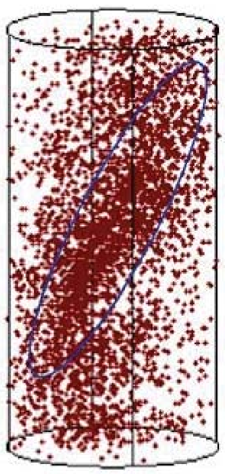

Spatial AE locations

Laboratory test

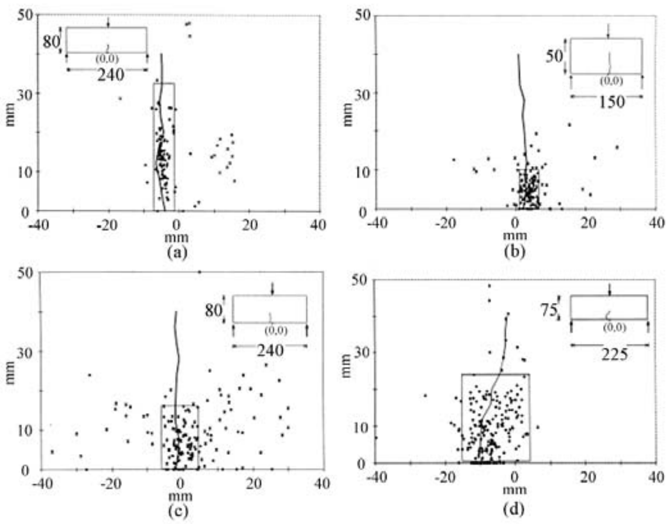

Spatial acoustic emission (AE) locations and experimental failure of red sandstone at a confining pressure of 35 MPa (Yang et al. 2012)

Acoustic emission (AE) locations and final macroscopic fracture pattern in the three-point bending test (a) Berea sandstone; (b) Sioux quartzite; (c) Charcoal granite; (d) Rockville granite (Zietlow and Labuz 1998)

20

Theories and approaches utilized

Linear elastic fracture mechanics

Stress intensity factor approach

Subcritical crack growth theory

Charles equation

Crack propagation schemes

Elasto-plastic stress redistribution

Subcritical crack growth simulation using Charles equation and celluar automate

$$t_{zone} = \int_{c_0}^{c_c} \frac{dc}{v}$$

$$c_c = min\left\{c_{I_c}, c_{II_c}, d_{zone}\right\} = min\left\{\frac{2}{\pi}\left(\frac{K_{I_c}}{\sigma}\right)^2, \frac{2}{\pi}\left(\frac{K_{II_c}}{\tau}\right)^2, d_{zone}\right\}$$

$$t_{zone} = \int_{c_0}^{c_c} \left[v(K_I) + v(K_{II})\right]^{-1} dc = \int_{c_0}^{c_c} \left[AK_I^n + AK_{II}^n\right]^{-1} dc$$

$$\begin{aligned} t_{zone} &= \frac{1}{A}\int_{c_0}^{c_c} \left[\left(\sigma\left(\frac{1}{2}\pi c\right)^{1/2}\right)^n + \left(\tau\left(\frac{1}{2}\pi c\right)^{1/2}\right)^n\right]^{-1} dc \\ &= \frac{1}{A\left(\sigma^n + \tau^n\right)}\left(\frac{2}{\pi}\right)^{n/2} \int_{c_0}^{c_c} c^{-n/2} dc \\ &= \frac{1}{A\left(\sigma^n + \tau^n\right)}\left(\frac{2}{\pi}\right)^{n/2} \frac{c_c^{1-n/2} - c_0^{1-n/2}}{1 - n/2} \end{aligned}$$

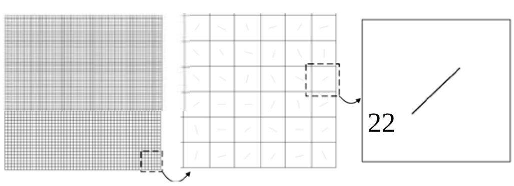

Konietzky, Heftenberger & Feige 2009

uniaxial
tension

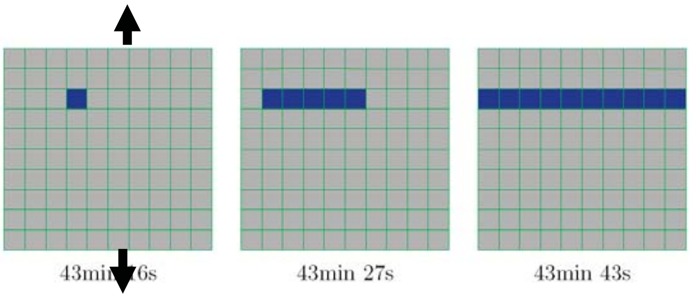

uniaxial
compression

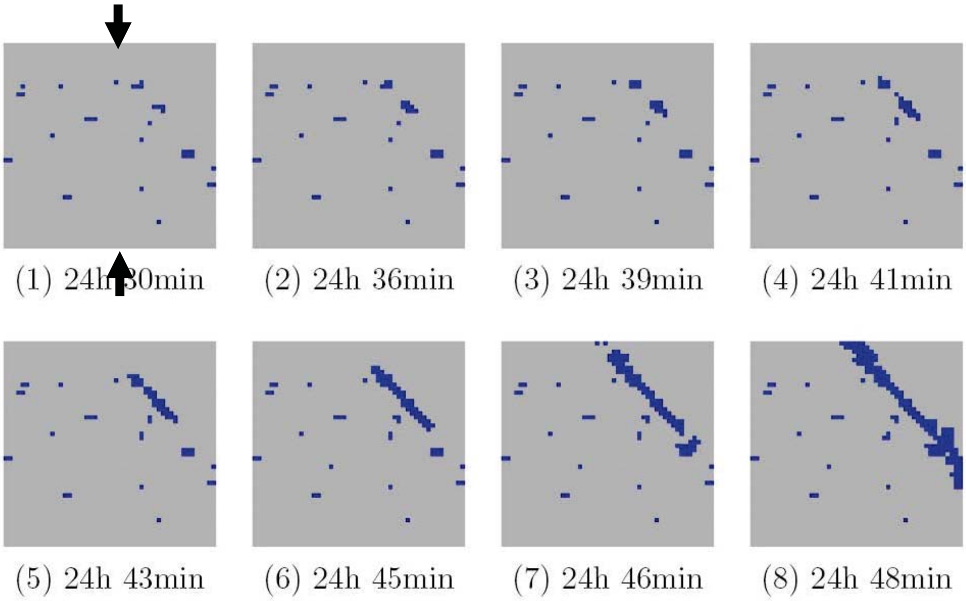

Typical damage development during uniaxial loading

Konietzky, Heftenberger & Feige 2009

Comparison: damage development under uniaxial compression and tension

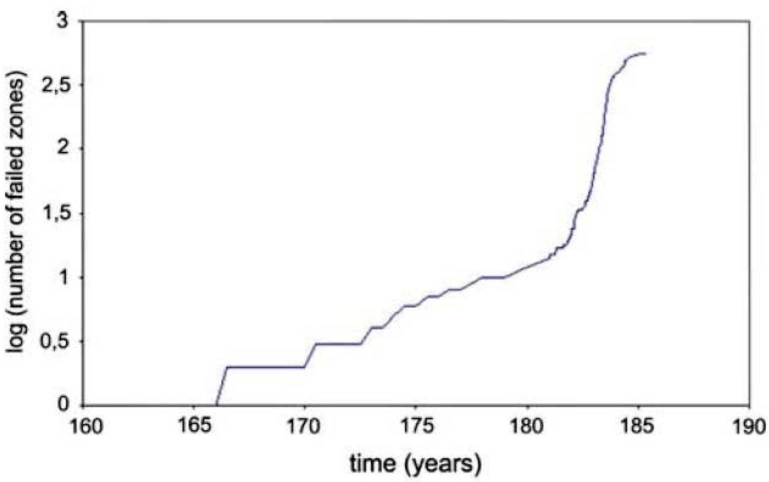

Compressive load

Same load magnitude !!

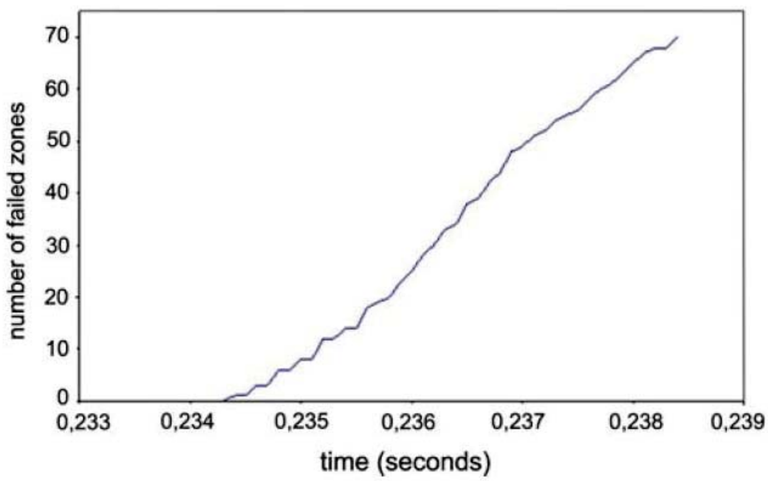

Tensile load

Zone size: 0.04 m;
Initial crack lengths:
normal distribution;
(Mean: 0.013 m, STD: 0.0001 m)
Initial crack orientations: uniform
distribution

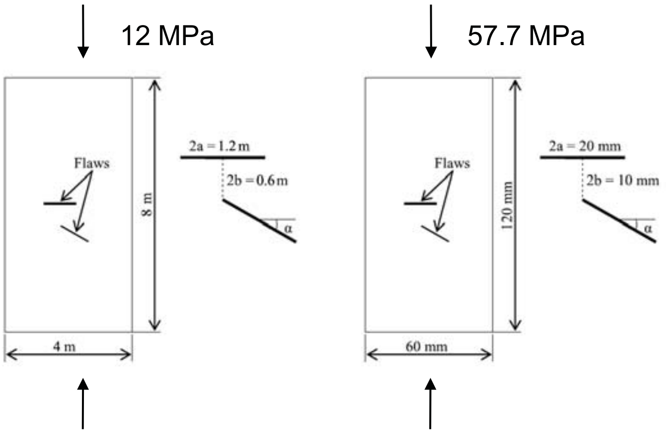

Hwangdeung granite (Lee and Jeon 2011)

30º | 45º | 60º

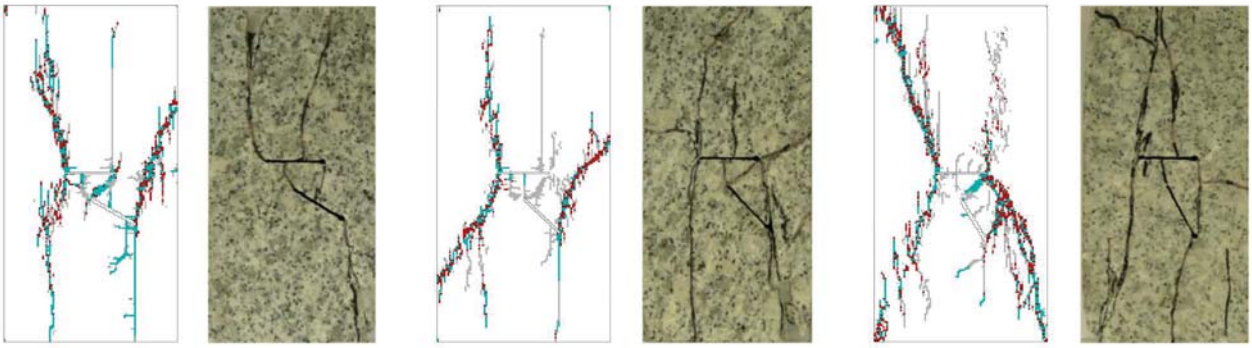

9.6e10 years | 9.0e10 years | 6.8e12 years

Li & Konietzky 2013

Practical Application: Pillar

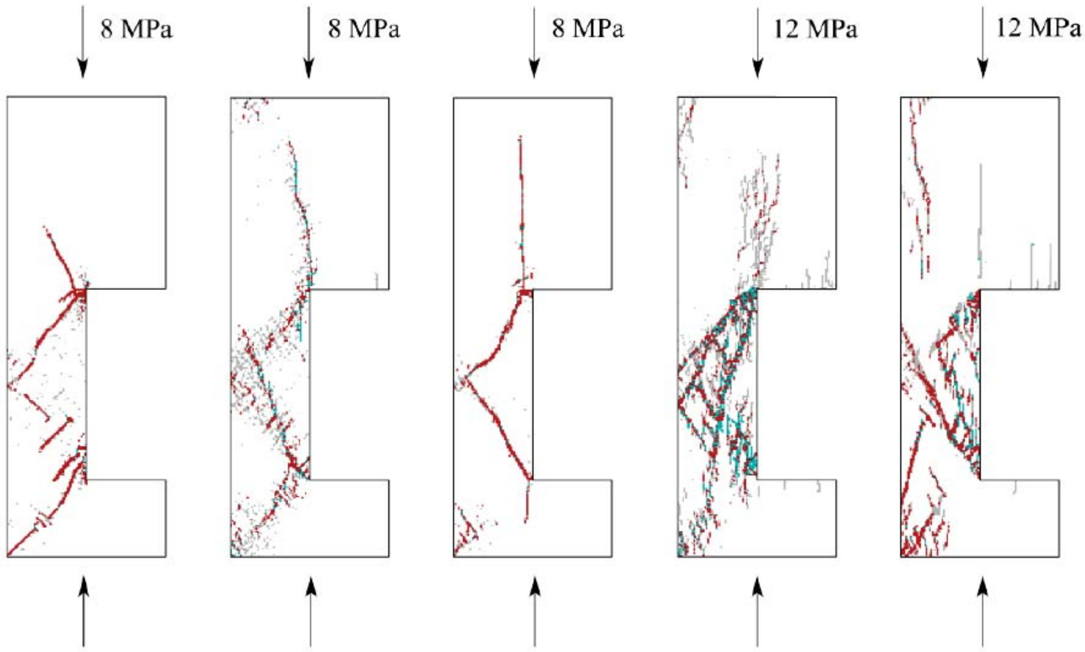

Basic model | Fixed orientation model | Wing crack model

18.7 s (a) | 610 y (b) | 2 d (c) | 2.6e7 y (d) | 6.6e7 y (e)

Li & Konietzky 2013

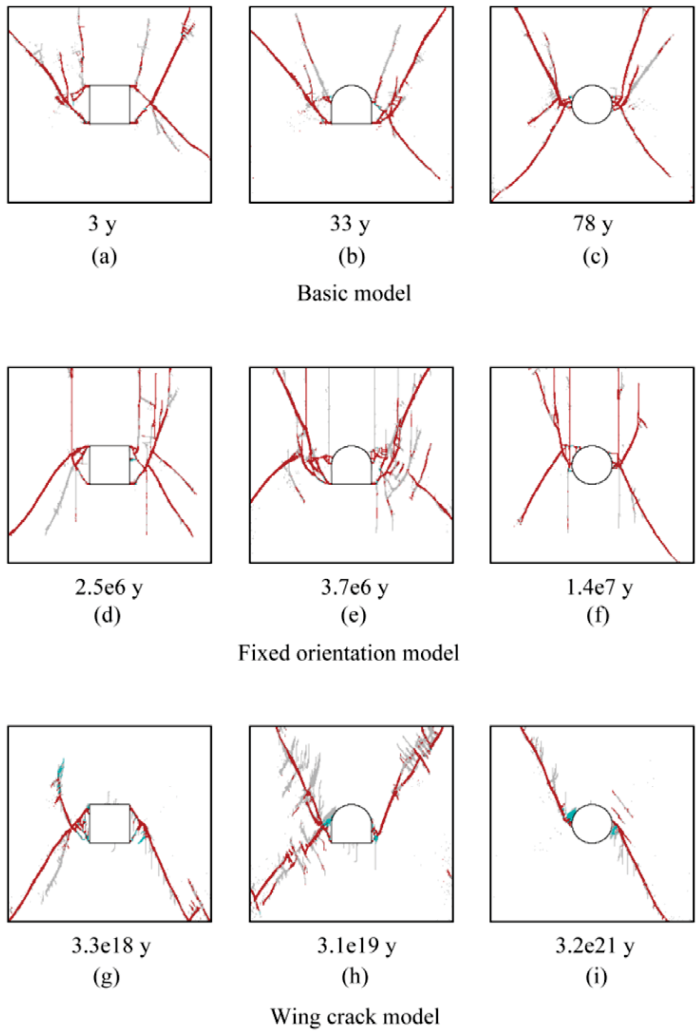

Practical Application: Tunnel , Drift

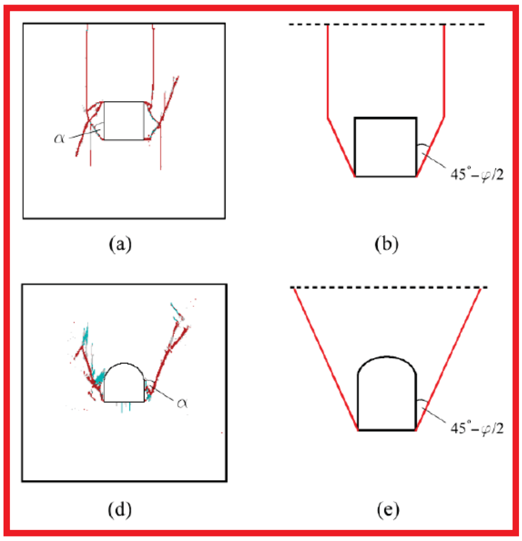

Li & Konietzky 2013

Model concepts

for

Opalinus clay

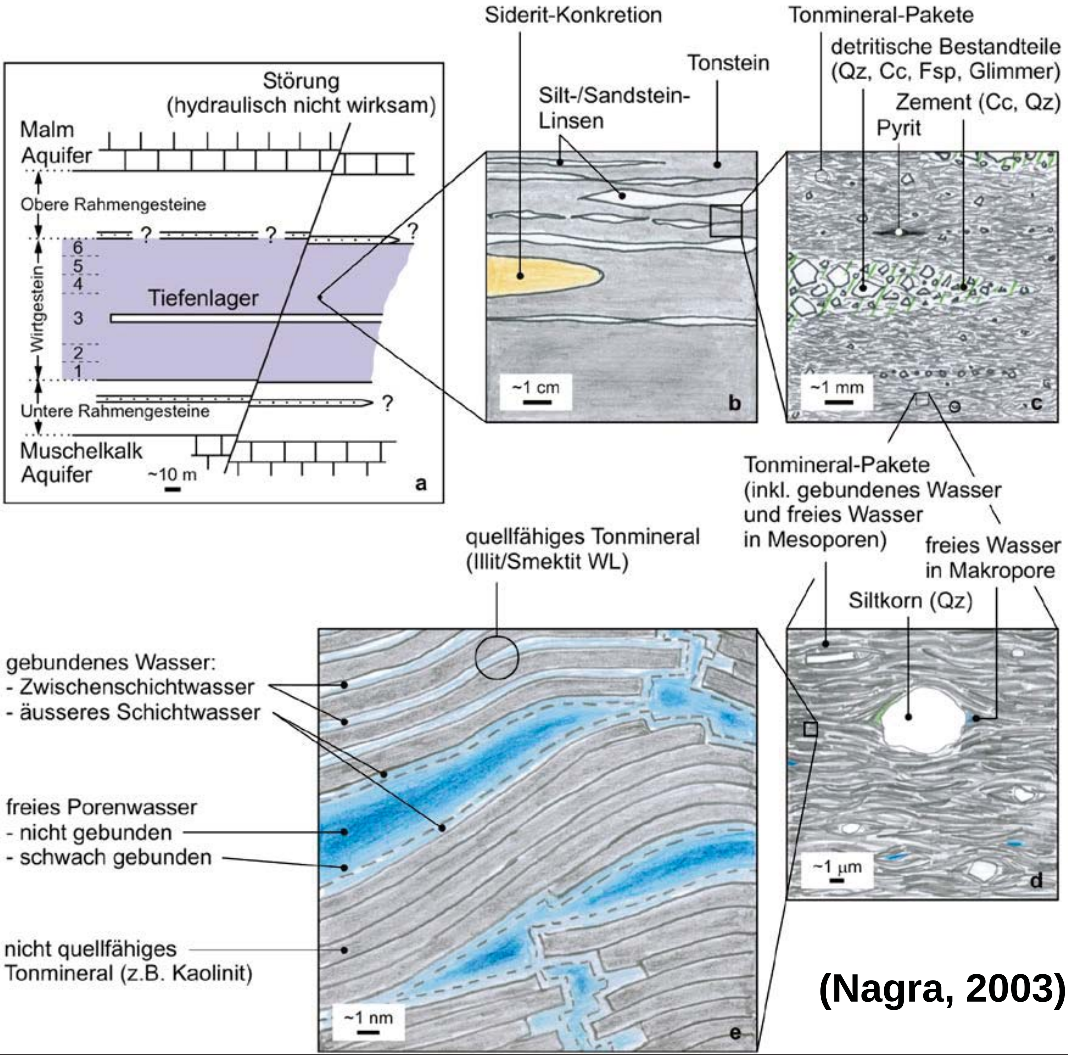

(Nagra, 2003)

29

2 concepts

„Phenomenological“ concept

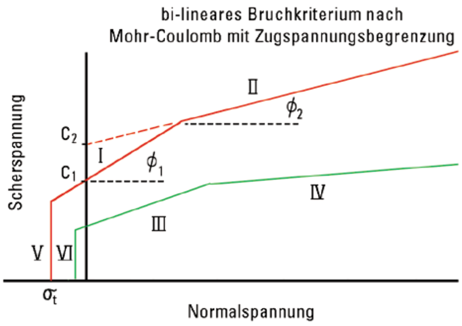

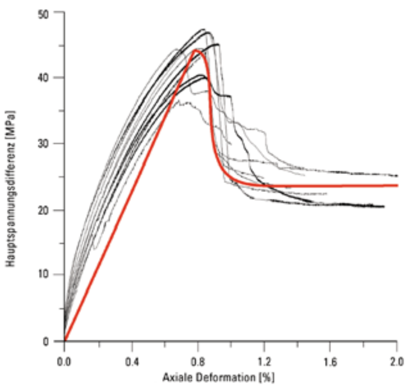

„Physical“ concept

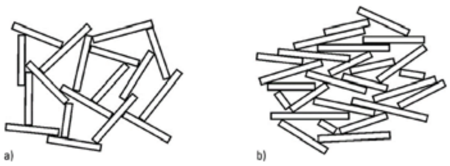

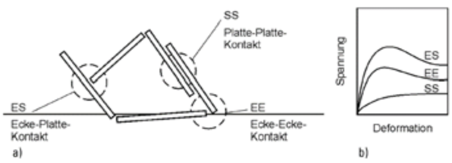

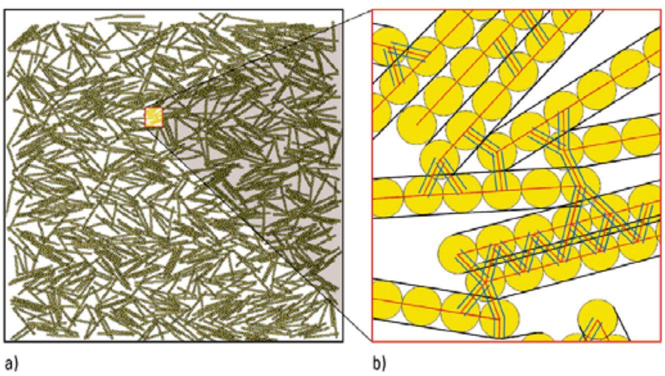

„Physical“ concept

at the micro-scale

31

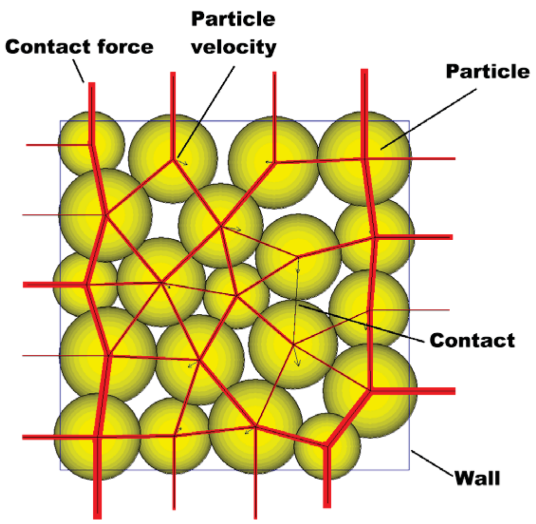

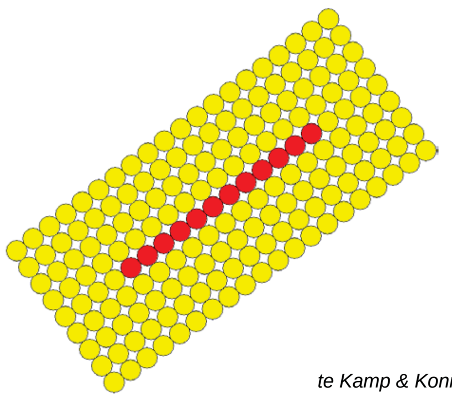

Numerical model
with clay plates, free water and
bounded water
(Lennard-Jones-Potential)

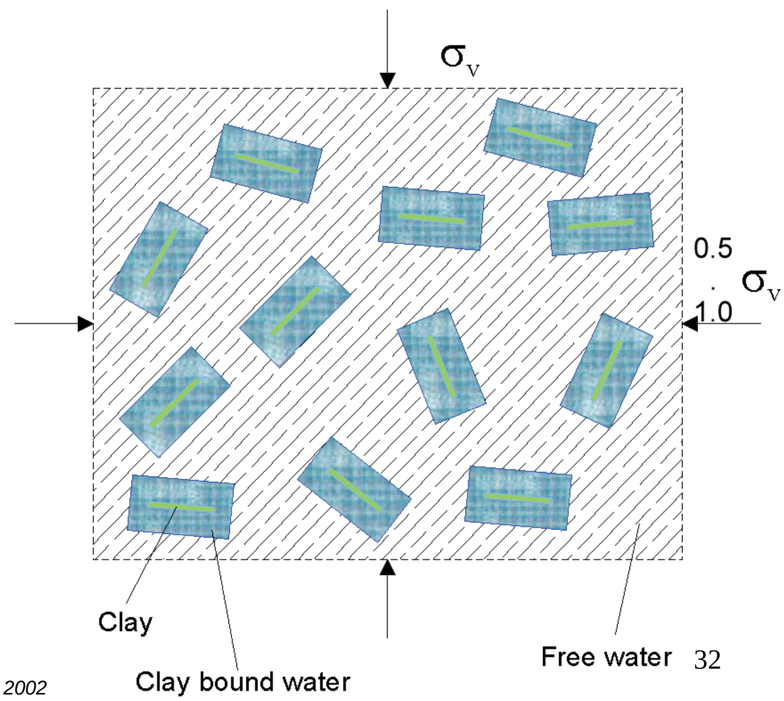

te Kamp & Konietzky 2002

32

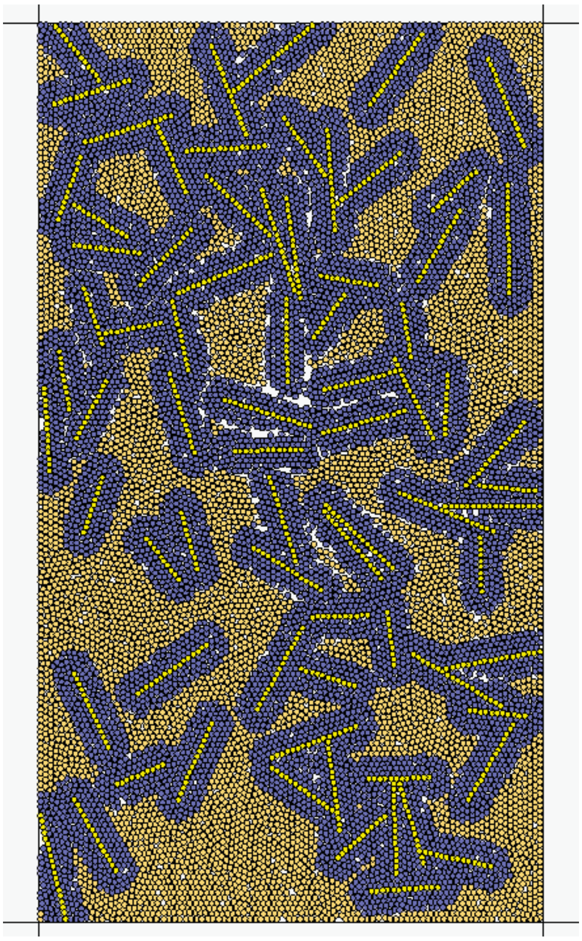

Model set-up

Initial state

Final state

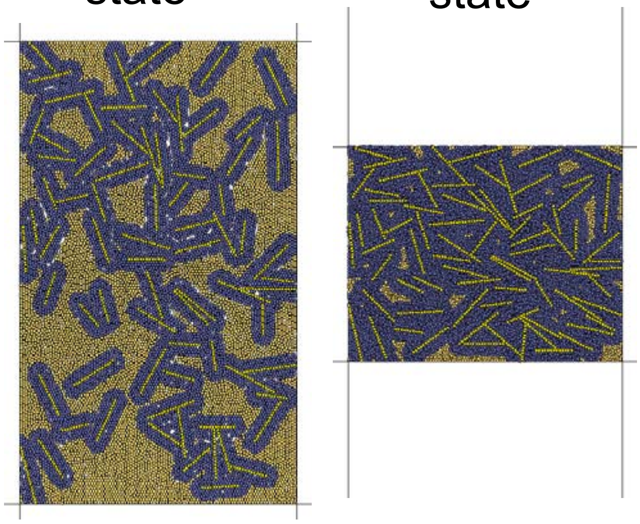

Compaction of saturated clay package under loading

Re-orientation of clay plates during compaction process

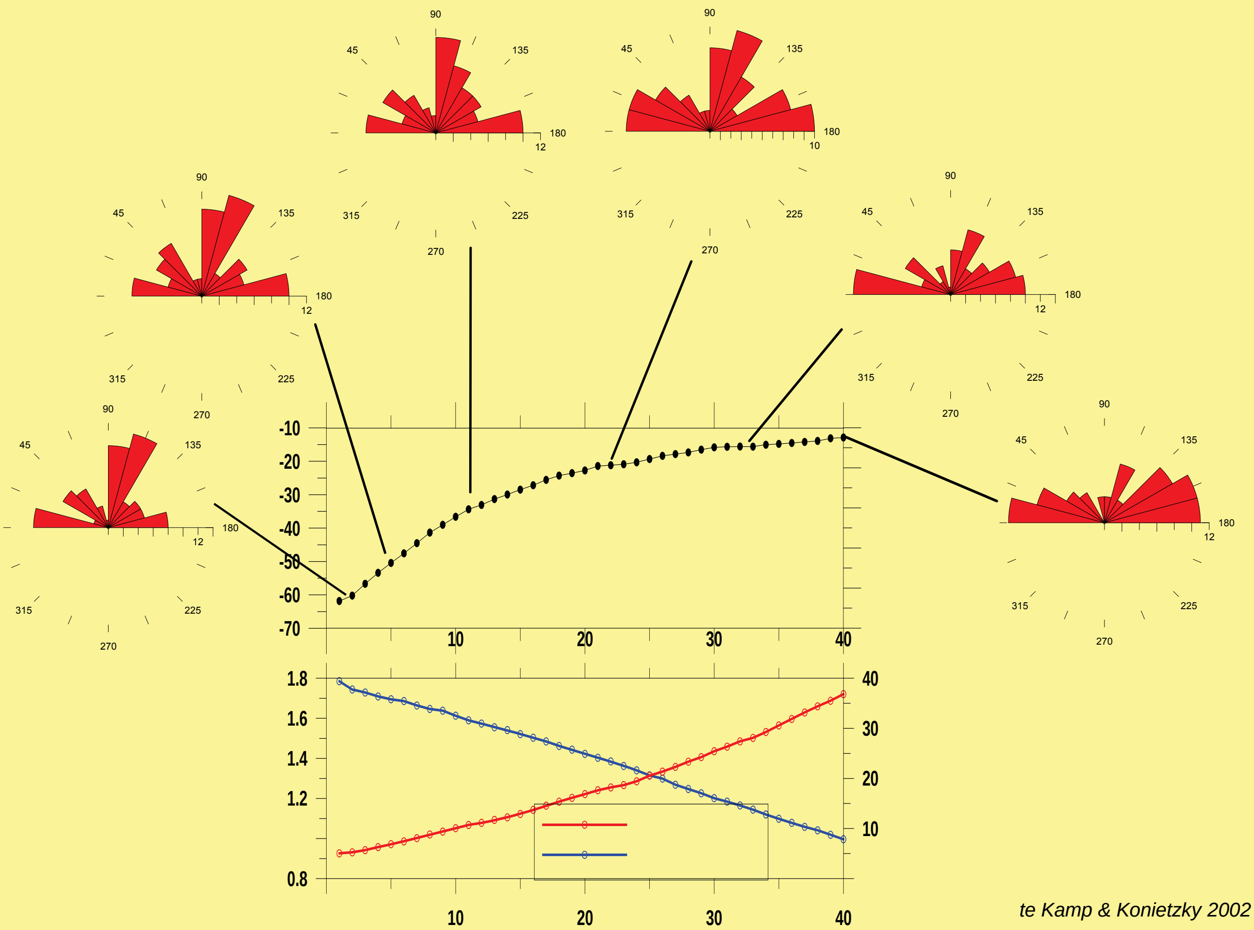

te Kamp & Konietzky 2002

Clay plate model without explicit consideration of water

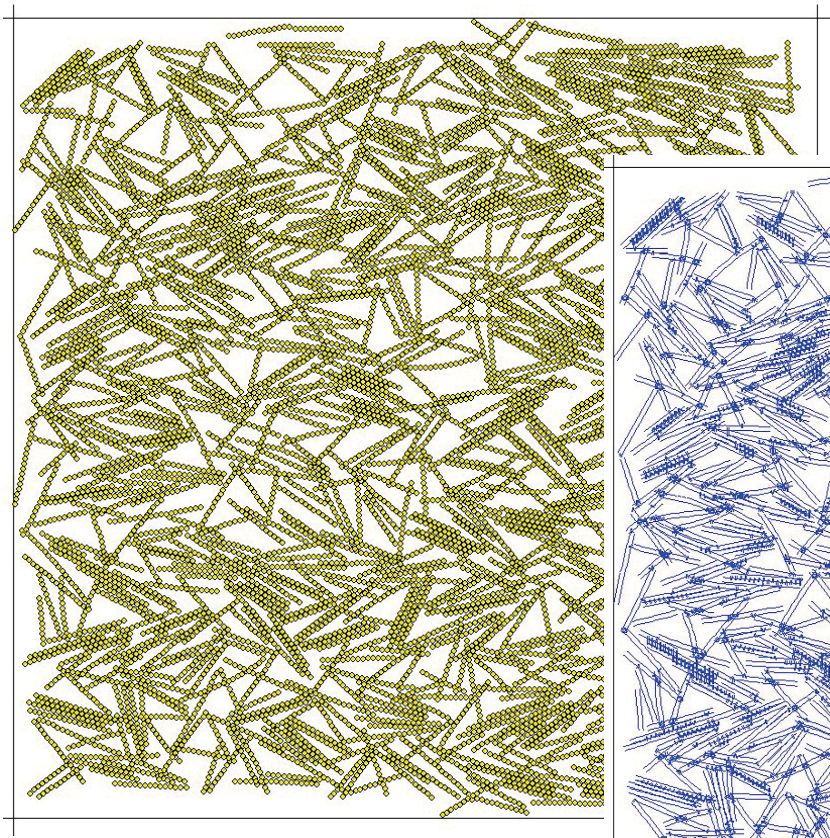

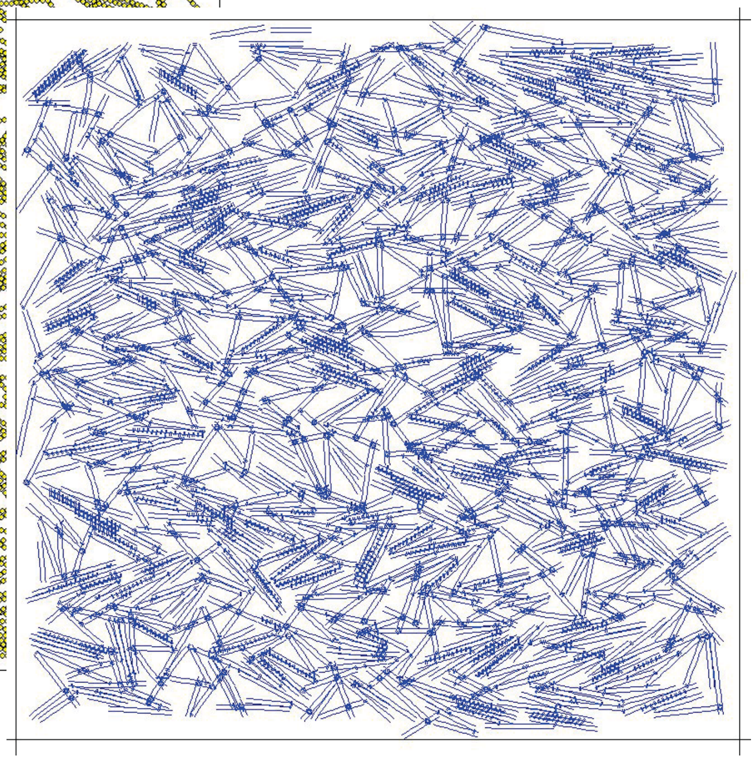

Porosity app. 50%

te Kamp & Konietzky 2002

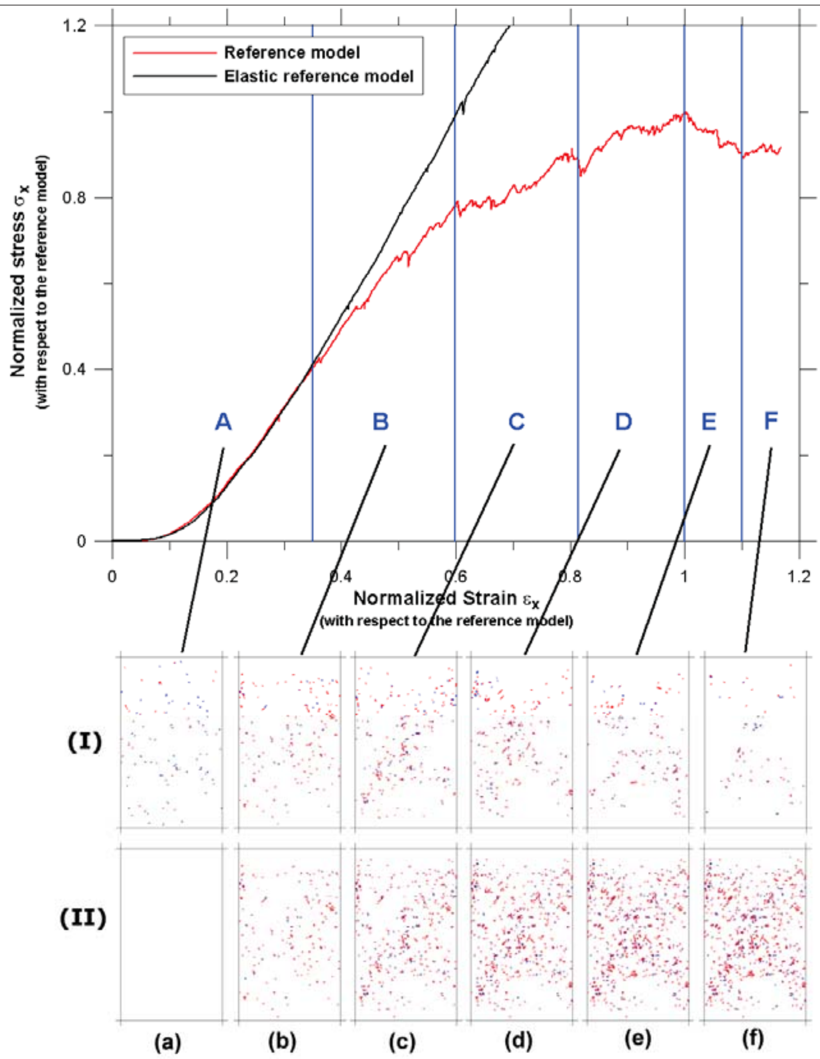

Stress strain behaviour and fracture pattern of numerical clay stone model

I: accumulated cracks

II: new cracks per phase

te Kamp & Konietzky 2002

Compaction under constant load levels
(note: irreversible plastic deformations)

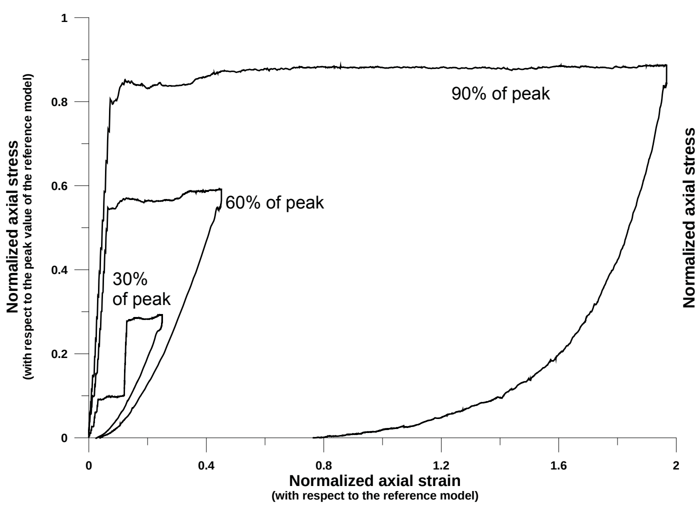

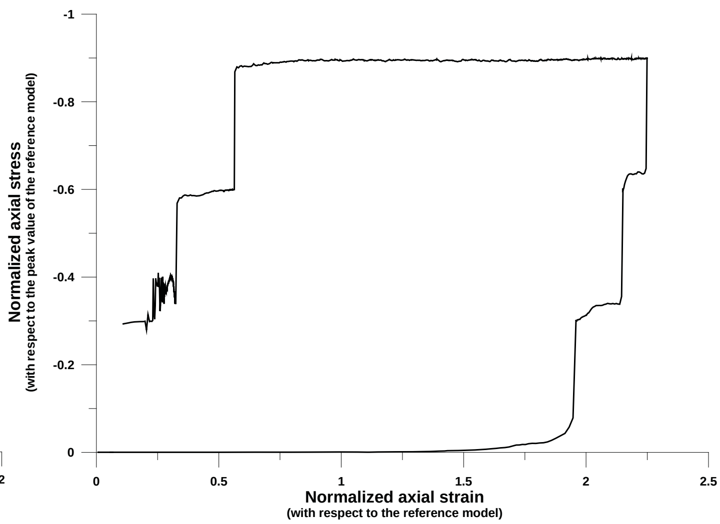

te Kamp & Konietzky 2002

„Physical“ concept

at the meso-scale

Anisotropic model for Opalinus Clay

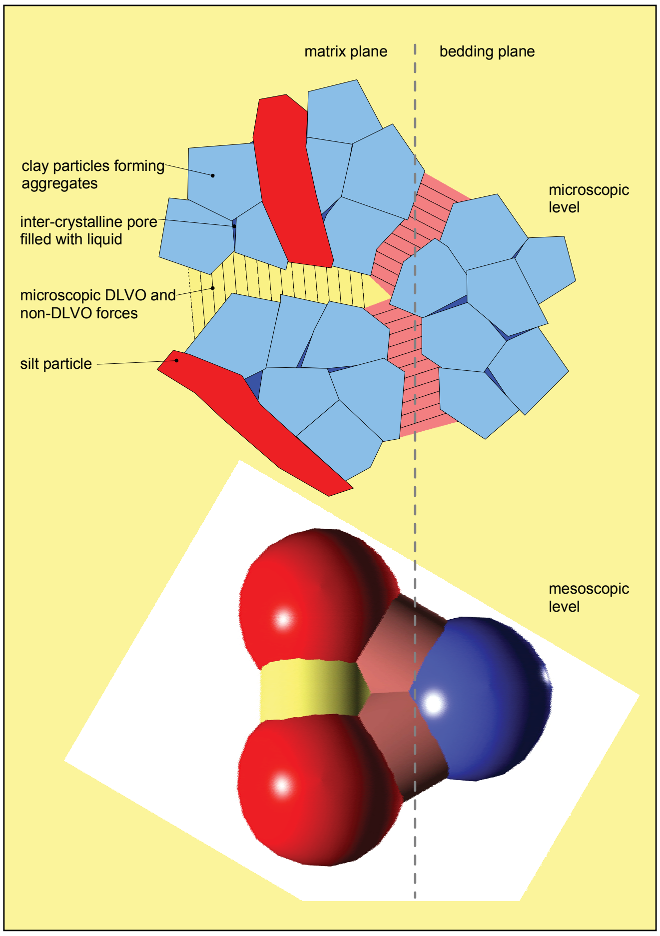

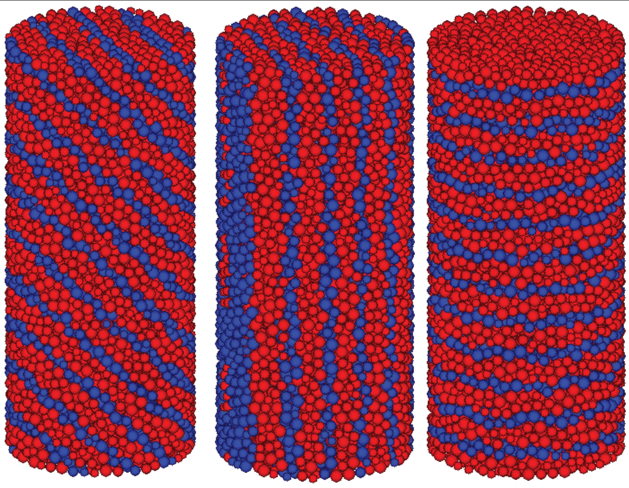

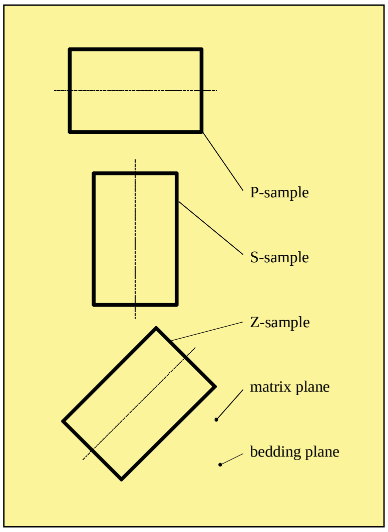

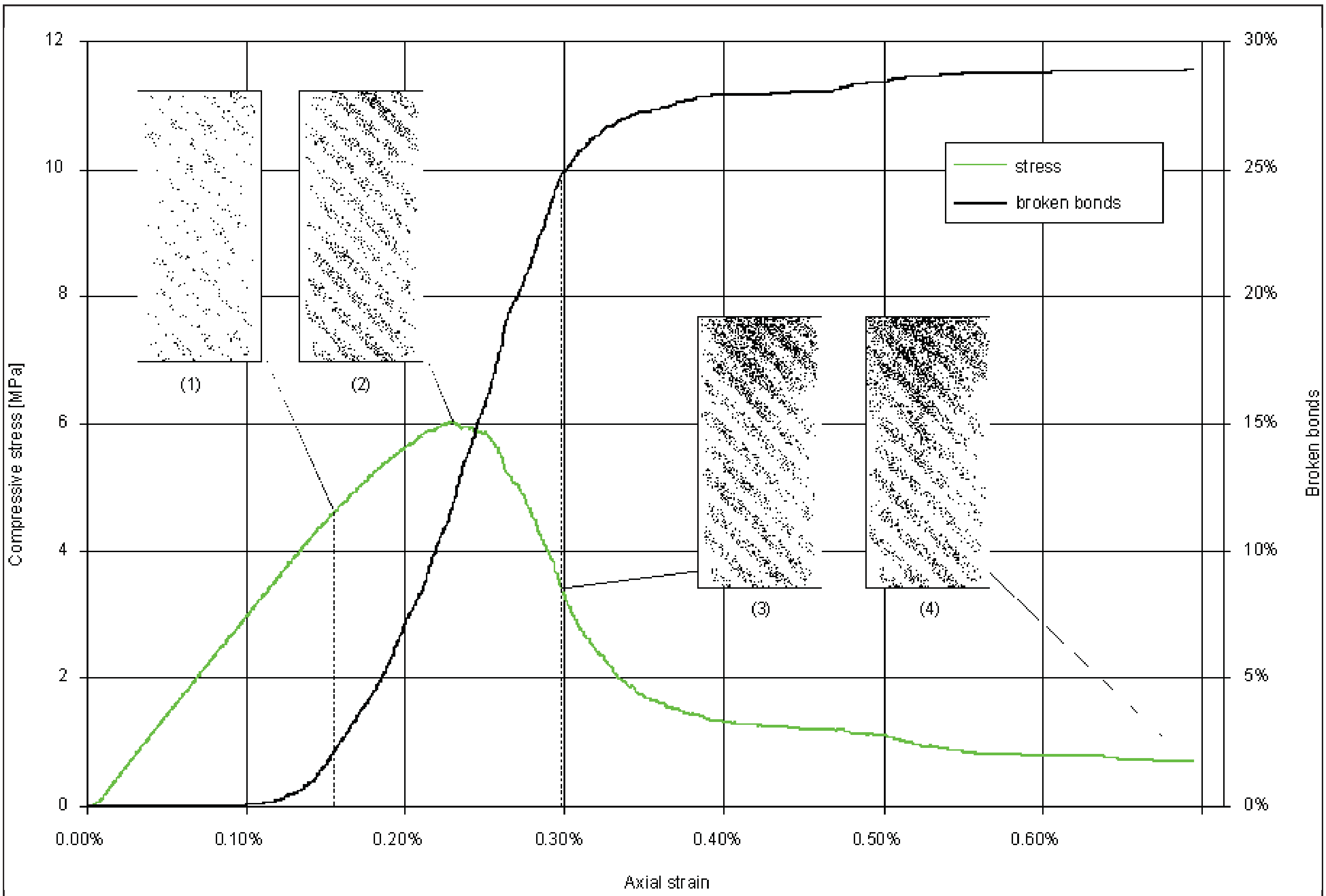

Stress – strain behaviour and fracture pattern: uniaxial compression test (S-Sample)

Uniaxial tensile testing: stress-strain curves and fracture pattern

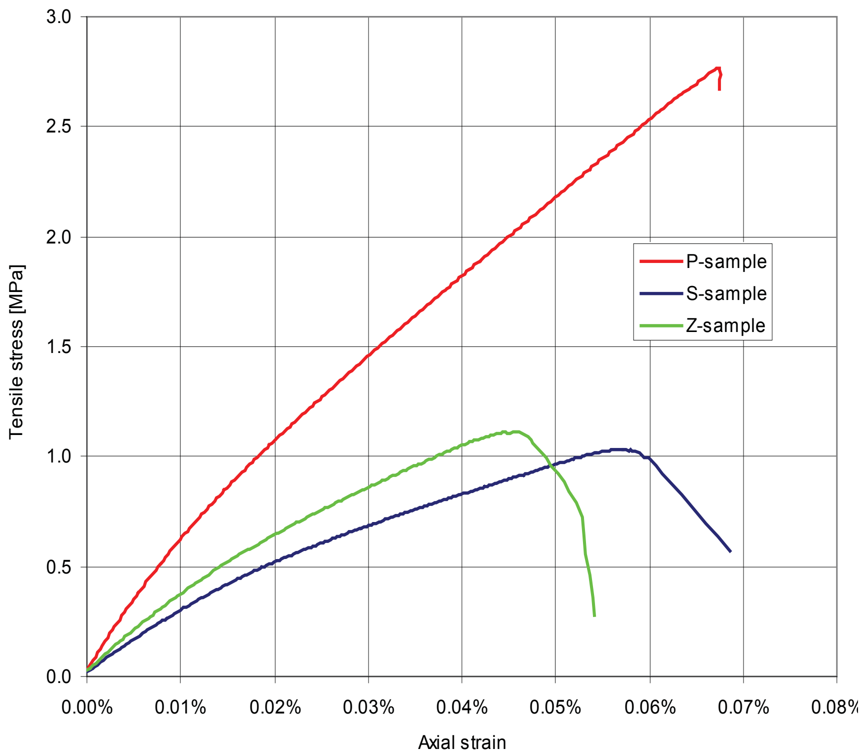

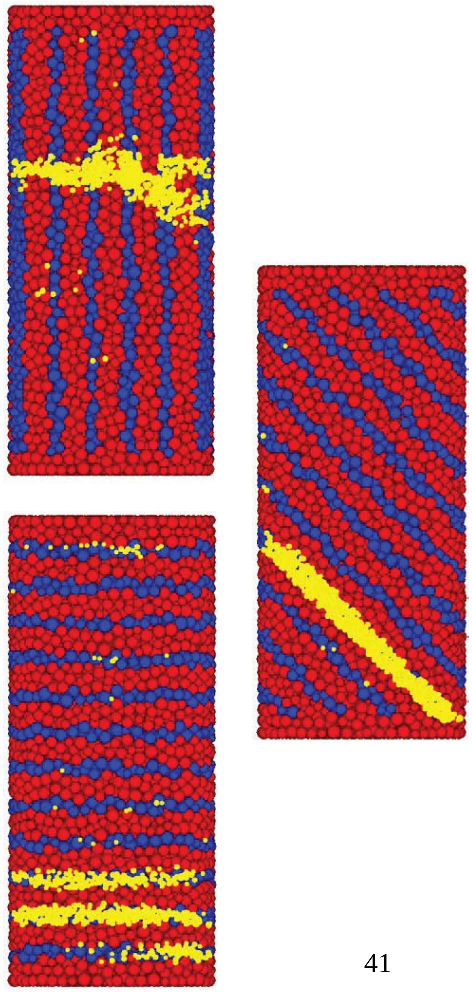

41

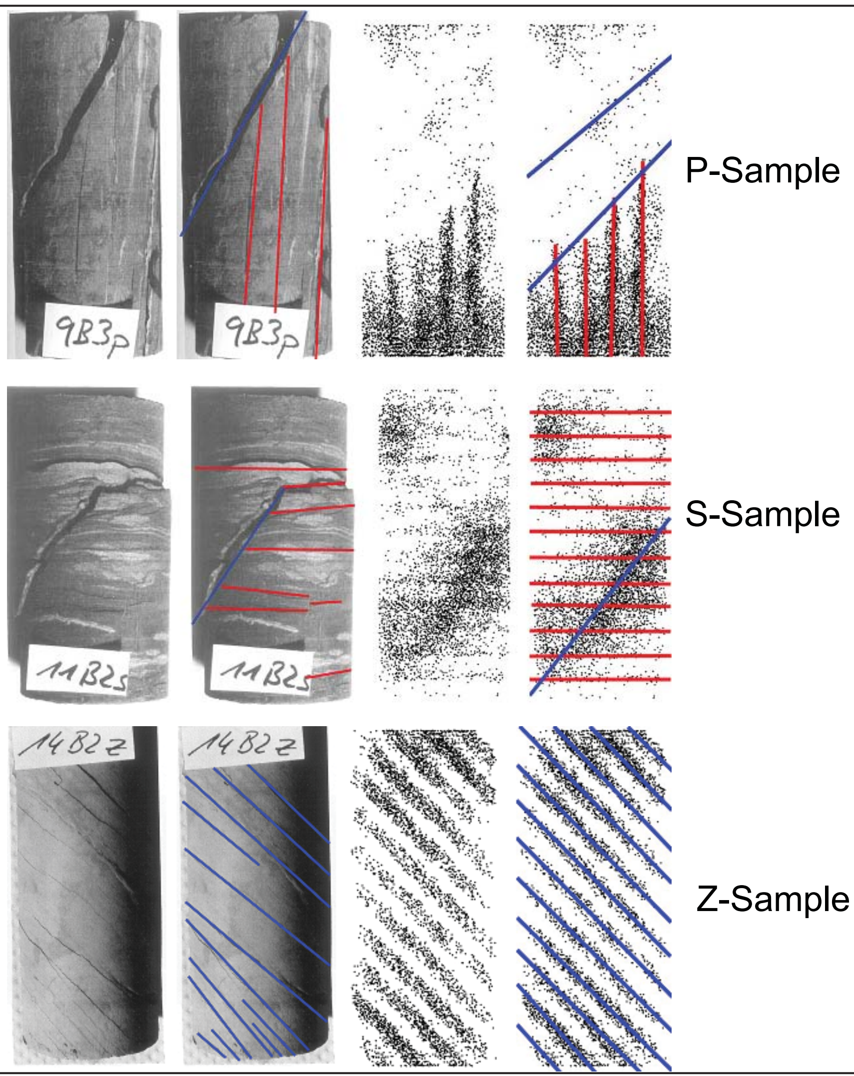

Uniaxial compression:

fracture pattern lab vs. model

42

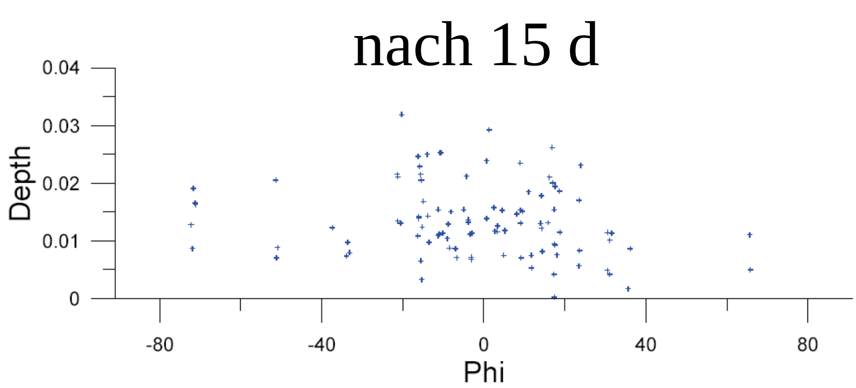

c) Développée du tunnel donnant les positions des micro-fractures (angle en °, profondeur en m)

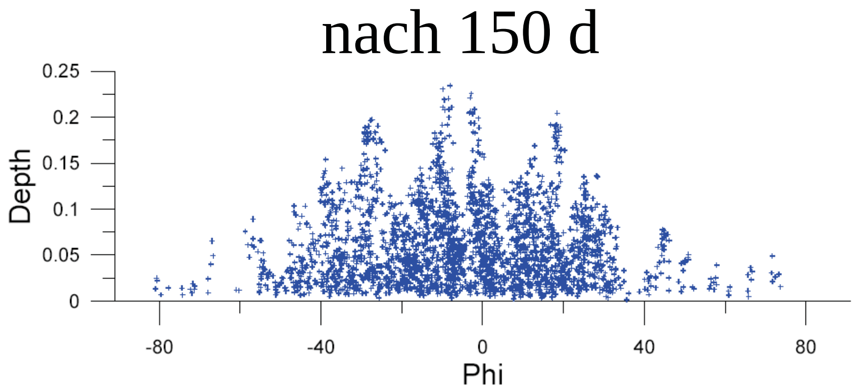

c) Développée du tunnel donnant les positions des micro-fractures (angle en °, profondeur en m)

EDZ:
fracture pattern as function of time

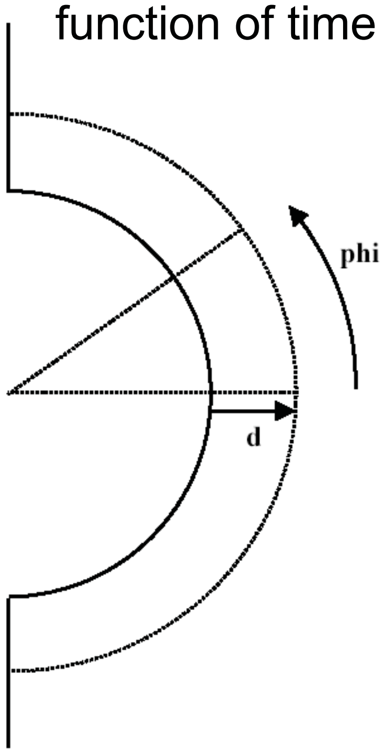

Permeability and flow area development in EDZ vs. time

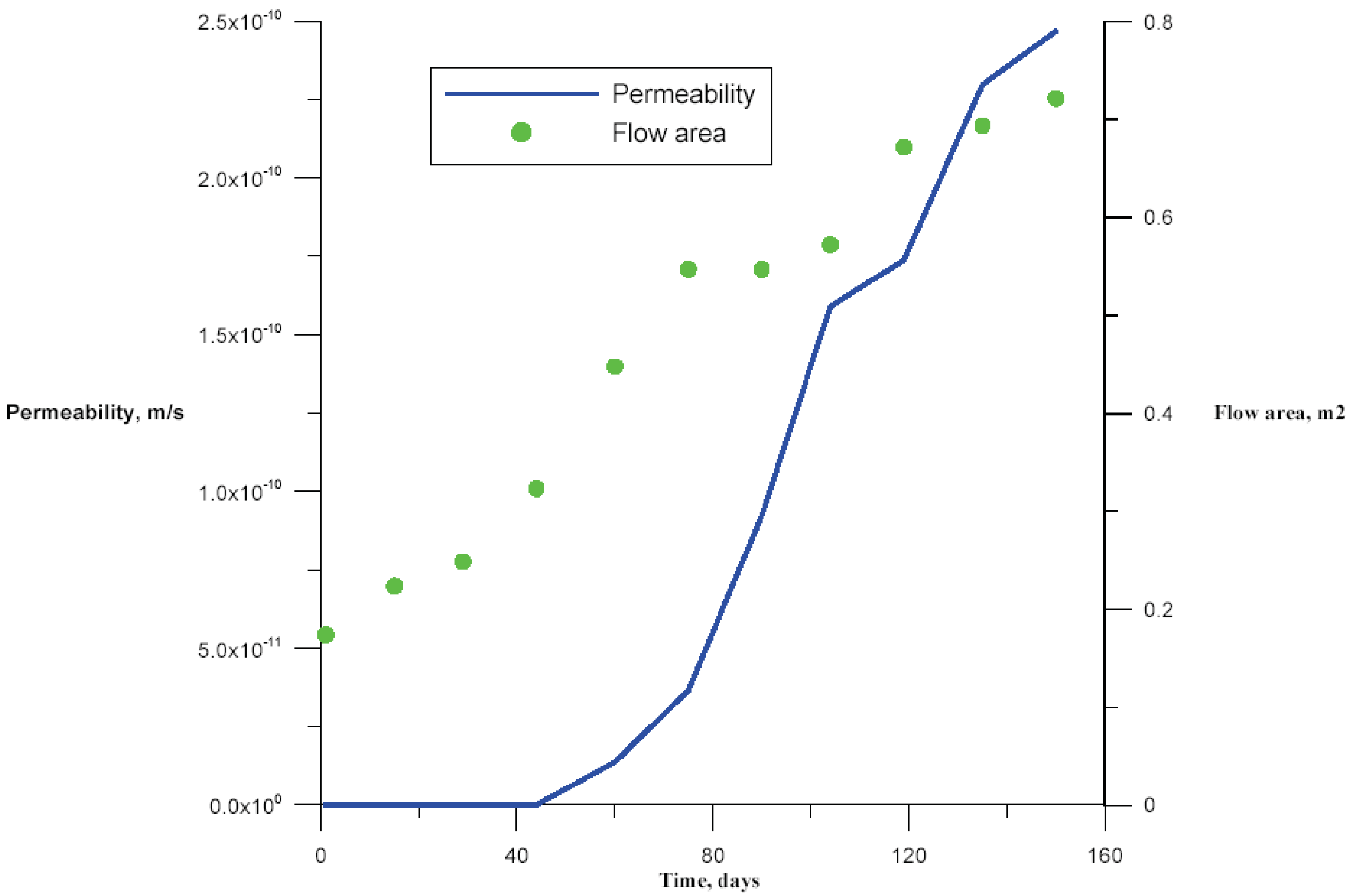

EDZ-study: Mt. Terri, tunnel radius = 1.8 m

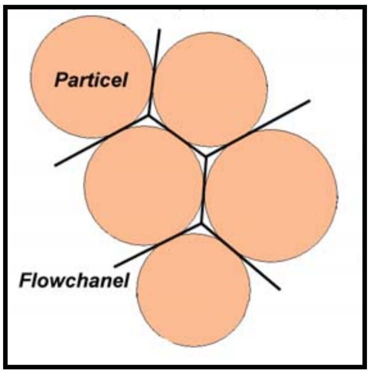

$$\Delta P = -K\frac{\Delta V}{V}$$

$$\dot{Q} = Ka^3\frac{\Delta P}{\Delta X}$$

$$a = \frac{a_0 F_0}{F + F_0}$$

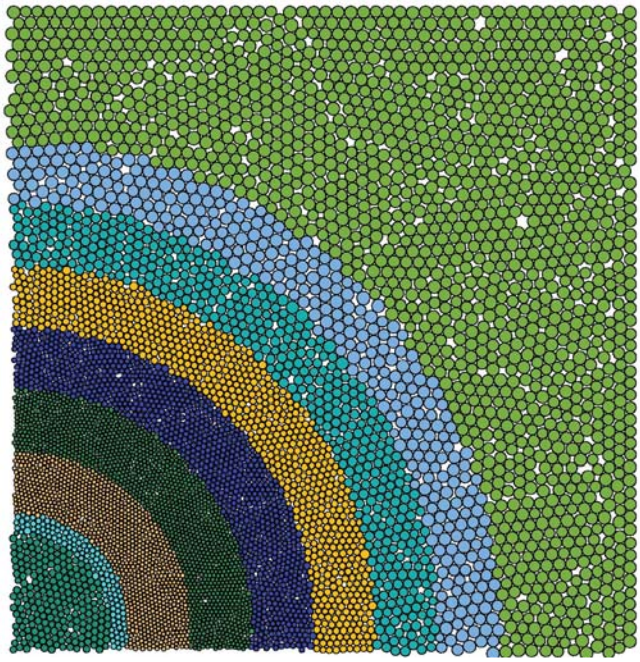

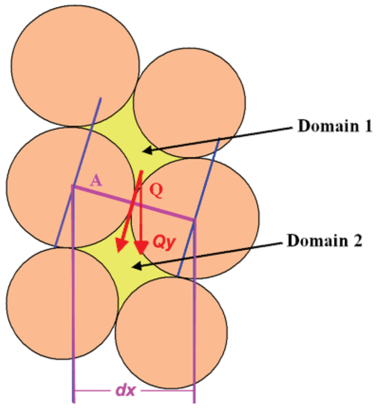

Numerical model set-up and
Ilustration of HM-coupling scheme

te Kamp, Konietzky & Blümling 1999
Konietzky, te Kamp & Blümling 2001

$P_{p,ini}$=2 MPa

1 day

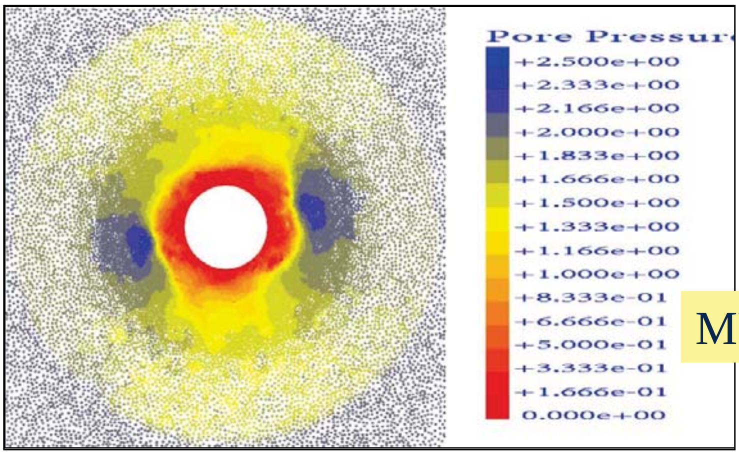

MPa

1 month

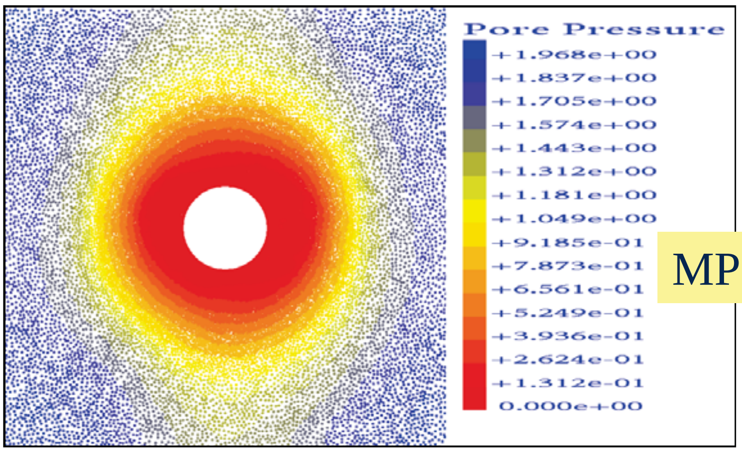

MPa

Pore pressure distribution around opening

te Kamp, Konietzky & Blümling 1999
Konietzky, te Kamp & Blümling 2001

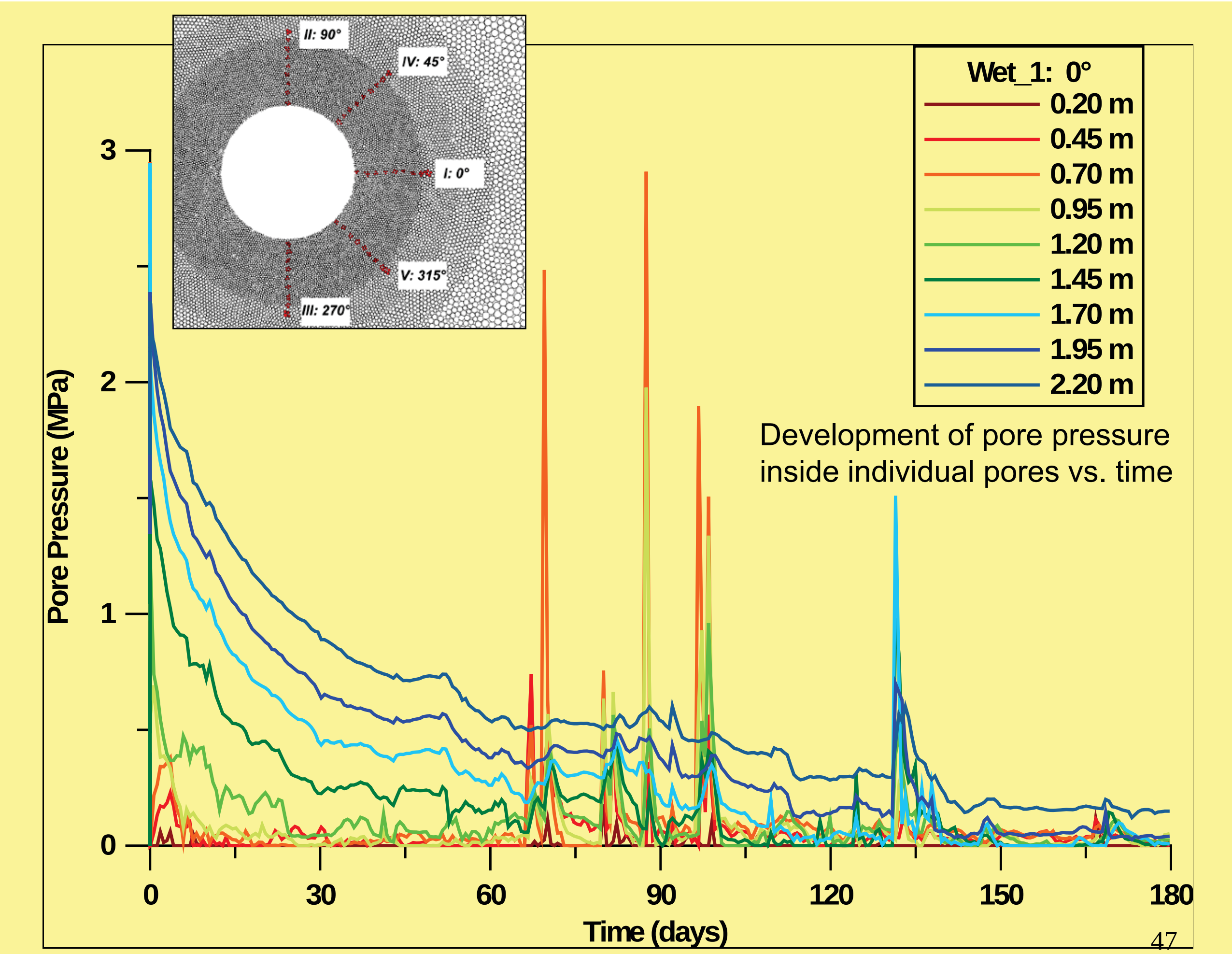

te Kamp, Konietzky & Blümling 1999
Konietzky, te Kamp & Blümling 2001

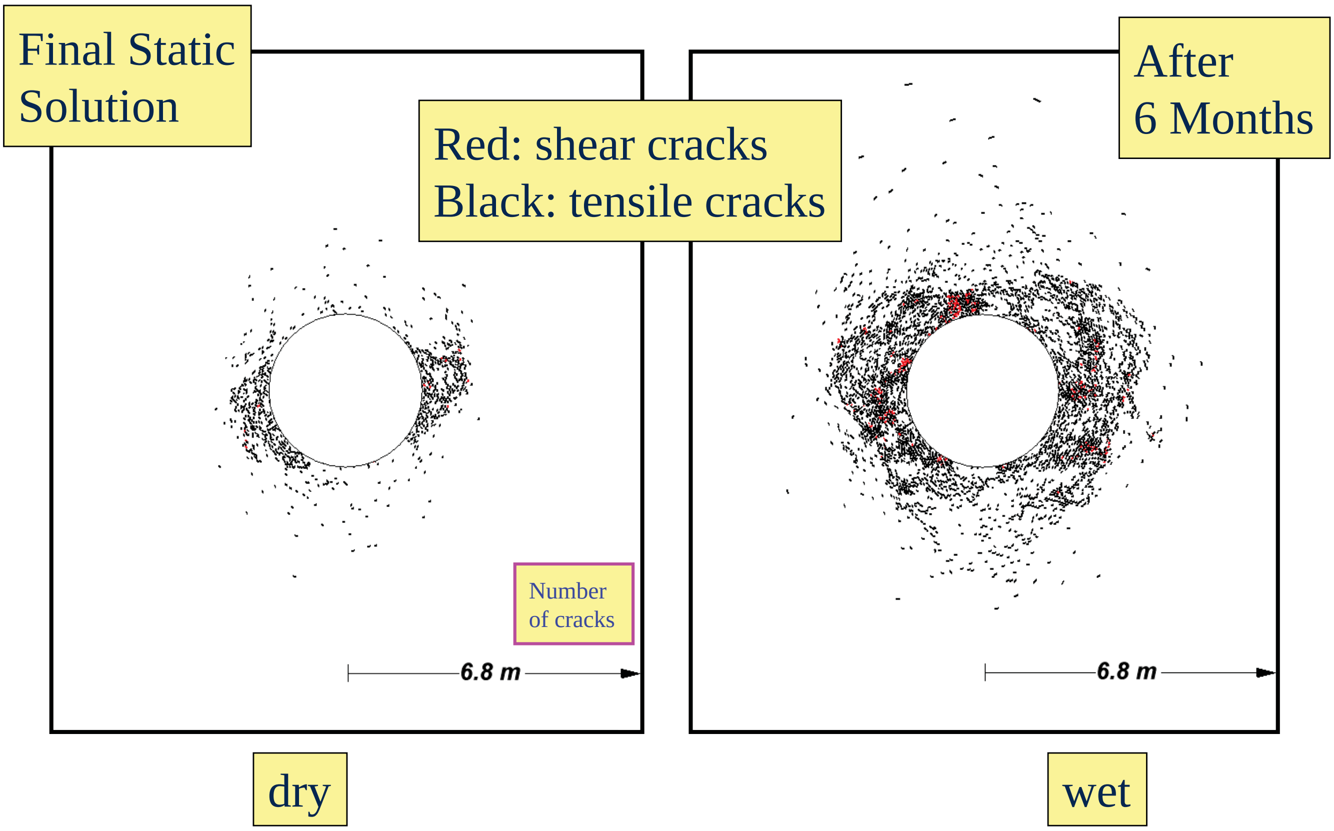

Comparison: damage state under dry and wet conditions

te Kamp, Konietzky & Blümling 1999
Konietzky, te Kamp & Blümling 2001

Simulation potential at the meso/macro-scale based on DEM technique

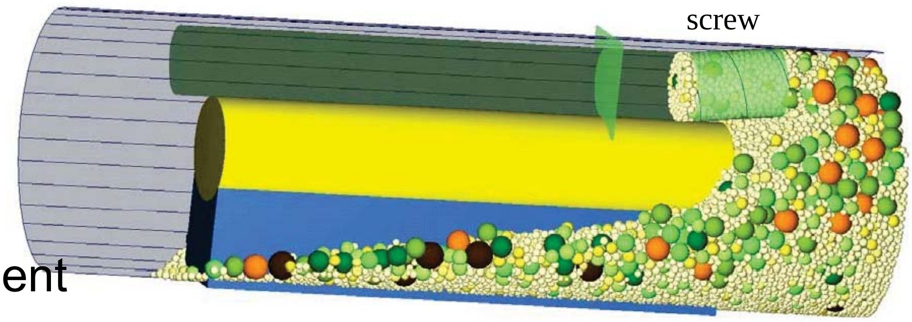

Fuller distribution

Emplacement of backfill

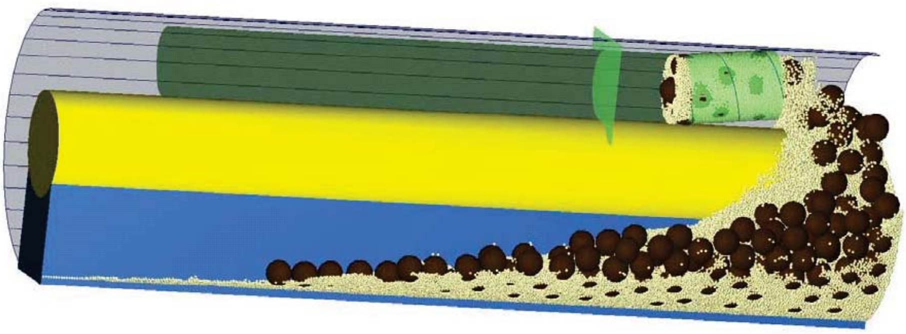

Bimodale size distribution

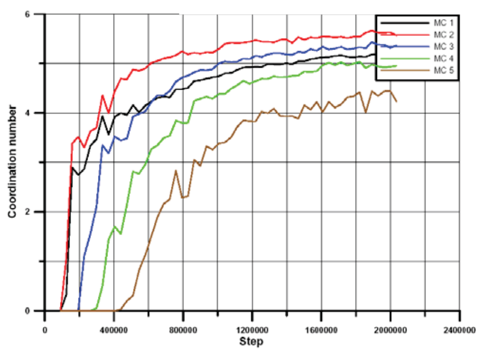

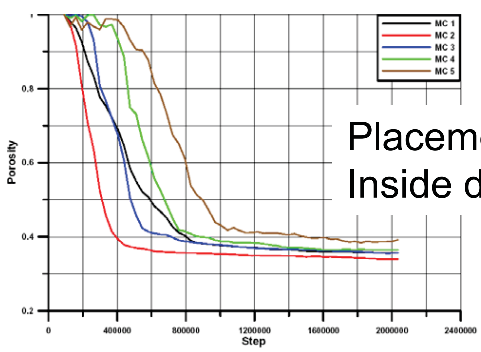

Placement of bentonite pellets
Inside drift with waste canister

Verständnis mikromech. Prozesse = Voraussetzung für fundierte Prognose

Knowledge micromech. Processes = Prerequisit for reliable Prediction

Correct micro- and meso-mechanical simulation demands the explicit consideration of:

- Grain shapes
- Grain size distribution
- Initial damage
- Intragranular and intergranular fracturing
- Porosity (shape, size, distribution)
- Mineral components / phases
- Critical and subcritical crack growth
- Simulation of granular flow and compaction

Korrekte mikro- und meso-mechanische Simulationen erfordern die explizitethe Berücksichtigung von:

- Kornform
- Korngrößenverteilung
- Initiale Schädigung
- Intragranulare und intergranul. Bruchprozesse
- Porosität (Form, Größe, Verteilung)
- Mineralbestand
- Kritisches und subkritisches Risswachstum
- Simulation of Partikelströmen und Kompaktion

Thanks for your kind attention

TU Bergakademie Freiberg
Institut für Geotechnik
Lehrstuhl Felsmechanik

Following co-workers have contributed to the presented results:
Dr. Li, Dr. te Kamp, Dr. Gröger, Dr. Tan, Mr. Baumgarten, Dr. Herbst, Dr. Groh